UNIVERSITY OF CALIFORNIA,
IRVINE

Optical Design Optimization for LED Chip Bonding and Quantum Dot based Wide Color Gamut Displays

DISSERTATION

submitted in partial satisfaction of the requirements
for the degree of

DOCTOR OF PHILOSOPHY

in Engineering

by

Gunwoo Kim

Dissertation Committee:
Professor Frank G. Shi, Chair
Professor Chin C. Lee
Professor James C. Earthman

2017

TABLE OF CONTENTS

LIST OF FIGURES

LIST OF TABLES

ACKNOWLEDGMENTS

I would like to express the deepest appreciation to my committee chair, Professor Frank G. Shi, who continually guided me through my in-depth understanding of the research field and my self-development of academic competence with his creative ideas, warm encouragement, and constructive criticism. Without his persistent help, this dissertation would not have been possible.

I would like to thank my committee members, Professor Chin C. Lee and Professor James E. Earthman for their time and efforts in serving as my dissertation committee member, and their valuable suggestions on my work.

In addition, I would like to thank my colleagues Dr. Yu-chou Shih, Dr. Yue Shao, Dr. Linjuan Huang, and Yuanhan Chen. As my seniors and colleagues, they provided generous help and suggestions on my research, from experiment trainings to technical discussions.

Last but not least, I'd like to thank my wife, Sunyoung, and my beloved daughters, Erin and Ellie, for their unlimited support, my parents, Kwang-seok Kim and Dr. Nam Hee Kim, and my sister Dr. Sooan Kim, for their unconditional love, along my pursuit of doctorate degree.

CURRICULUM VITAE

2002-04	Taff System Co., LTD., Korea
2007	B.S. in Materials Science and Engineering, Hanyang University
2007-10	Samsung Electronics Co., LTD., Korea
2012	M.S. in Materials Engineering, University of Southern California
2017	Ph.D. in Engineering, University of California, Irvine

FIELD OF STUDY

Optical Packaging Design for Optoelectronic Devices

PUBLICATIONS

G. Kim, Y. C. Shih, and F. G. Shi, “Optimal Design of a Quantum Dot Color Conversion Film in LCD Backlighting,” IEEE Journal of Selected Topics in Quantum Electronics, vol. 23, no. 5, pp. 1-4, 2017.

Y.-C. Shih, G. Kim, J.-P. You et al., "LED Die Bonding," Materials for Advanced Packaging, D. Lu and C. P. Wong, eds., pp. 733-766, Cham: Springer International Publishing, 2017

Y.-C. Shih, G. Kim, J.-P. You and F. G. Shi, "Printable optically transparent adhesive processing for bonding of LED chips to packages," Materials Science in Semiconductor Processing, vol. 56, pp. 155-159, 2016.

Y.-C. Shih, G. Kim, J.-P. You and F. G. Shi, "Optical Interaction Between LED Backside Reflectors and Die Attach Adhesives," IEEE Photonics Technology Letters, vol. 28, no. 13, pp. 1446-1449, 2016.

G. Kim, Y.-C. Shih and F. G. Shi, “Optical Role of Die Bonding for Chip-on-Board White Light Emitting Diode Emitters,” IMAPS International Symposium on Microelectronics 2016

G. Kim, Y.-C. Shih, J.-P. You and F. G. Shi, “Optical role of die attach adhesive for white LED emitters: light output enhancement without chip-level reflectors,” Journal of Solid State Lighting, vol. 2, no. 1, pp. 1-8, 2015.

Y. Shao, Y. C. Shih, G. Kim, and F. G. Shi, "Study of optimal filler size for high performance polymer-filler composite optical reflectors," Optical Materials Express, vol. 5, pp. 423-429, 2015.

Y. C. Shih, G. Kim, L. Huang, J. P. You, and F. G. Shi, "Role of Transparent Die Attach Adhesives for Enhancing Lumen Output of Midpower LED Emitters with Standard MESA Structure," IEEE Transaction on Component, Packaging, and Manufacturing Technology, vol. 5, pp. 731-736, 2015

Y. Shao, Y.-C. Shih, G. Kim and F. G. Shi, "Filler size dependence of optical reflectance for polymeric-filler reflectors," Electronic Components and Technology Conference 2015

PATENTS

S. Lee, J. Park, D. Cho, H. Cho, G. Kim, "MEMS shutter and display apparatus having the same", Patent No. 8,817,353, Aug. 26, 2014

S. Yoon, G. Kim, J. Park, H. Cho, "Micro-shutter and display apparatus having the same", Patent No. 8,462,416, Jun. 24, 2013

H. Park, J. Park, D. Cho, J. Byun, S. Hong, Y. Kim, S. Yoon, G. Kim, S. Lee, "Field emitting device and display apparatus having the same," Patent No. 8,008,848, Aug. 30, 2011

G. Kim, J. Park, D. Cho, H. Park, J. Byun, J. Shin, S. Yoon, S. Hong, "Light emitting diode, backlight assembly having the same and method thereof," Patent No. 7,819,539, Oct. 26, 2010

J. Shin, J. Park, J. Kang, G. Kim, Y. Kim, H. Kim, H. Jang, "Lamp, method for manufacturing the same and liquid crystal display apparatus having the same", Pub. No. US2010/0128203 A1, May. 27, 2010

ABSTRACT OF THE DISSERTATION

Optical Design Optimization for
LED Chip Bonding and Quantum Dot based Wide Color Gamut Displays

By

Gunwoo Kim

Doctor of Philosophy in Engineering

University of California, Irvine, 2017

Professor Frank G. Shi, Chair

Light Emitting Diodes (LEDs) are the most beneficial optoelectronic devices for human lives. LEDs already dominated mainstream lightings market, not only the general lightings but also displays, medical applications, and so on, to replace conventional light sources due to their small forma factors and high efficiency. Extensive researches have been carried out ever since introduced, and reported significant enhancement in optical output for the individual LED chip, and it is also pointed out that the enhancement in optical output for the emitter and the lighting system level must be considered by improvement of packaging materials and processes. In addition, the requirement for wide color gamut as well as enhanced optical output has been more important to be applied for color displays such as liquid crystal displays (LCDs). This dissertation is focused on addressing two parts, to propose optimized packaging designs of LED emitters and displays based on the points mentioned above.

First, optimized designs of packaging materials and process of enhancement in optical output of individual LED emitters is proposed using transparent die bonding material considering optical characteristics. It is shown that the optically transparent die attach adhesive prevent light absorption from the LED chip so that a substantial amount of light output of blue and phosphor converted white LED emitters compared to the conventional LED emitters using silver (Ag) based die bonding material. This optimization includes surface mount device (SMD) and chip-on-board (COB) type LED emitters. In addition to the COB-LED emitters, a transparent substrate is also shown to enhance light output and able to form an omnidirectional LED emitter.

Second, optimized packaging designs for color conversion film are proposed for wide color gamut displays. It is shown that the converted peak wavelengths by using quantum dot (QD) materials from blue backlights are well tuned and matched with required color coordinates for LCDs with a wide color gamut. A dichroic filter applied on the color conversion film dramatically reduced the amount of QD materials required by recycling excessive blue emission. More advanced packaging design for the color conversion film as pixels is also studied to replace color filters not only for LCDs but also for OLEDs.

CHAPTER 1

BACKGROUND AND INTRODUCTION

1.1. BACKGROUND

The light emitting diode (LED) is one of the solid state lighting (SSL) technologies which has been dramatically improved for last three decades [1]. The LED technologies have opened the possibility of white light source by combining gallium nitride (GaN) based blue LED chip technology with phosphors, and have started to attract attention as a strong candidate to replace existing light sources [2, 3]. In the early stages of development, however, the manufacturing cost of the LEDs was relatively expensive compared to the conventional light sources despite the advantages such as high efficiency, ease of selecting peak wavelengths, small form factors and low power consumption. This issue has been a major obstacle for the LEDs to dominate the lightings market. After the extensive researches for decades, the price-over-power efficiency ($ / lumen) of the LEDs has become almost doubled up for the past five years (Figure 1.1), thus the LED-based lighting devices are rapidly penetrating the lightings market and increasing the portion as shown in Figure 1.2, and this tendency includes backlights for displays, industrial lightings, bio-medical applications, and even the general lightings [4, 5]. However, the LED-based lighting devices have not been fully

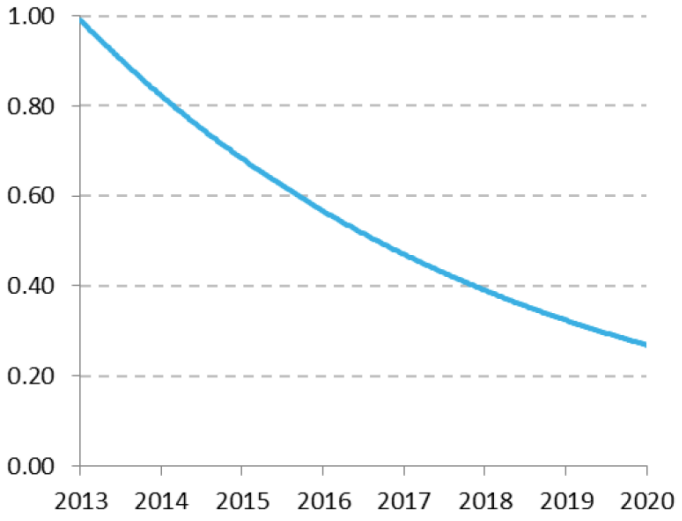

Figure 1.1. Relative cost for LED 800 lm A19 Lamp

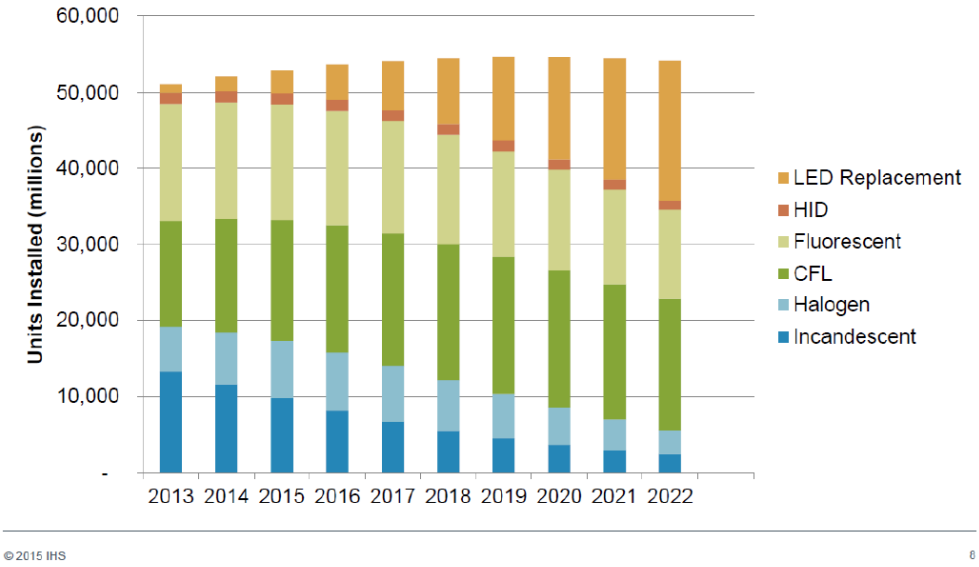

Figure 1.2. Evolution of the Global Installed Lamp Base by Lighting Technology

replaced in many applications yet. Figure 1.3 presents the penetration rates of LED lighting applications, and only a few applications such as traffic lightings and exit signs are replaced with LEDs almost 100 %, and the LEDs have only penetrated less than 20 % for most of applications. In terms of the energy saving, it is evident that the more applications to be replaced with LED-based light sources, with consideration of fixtures and infrastructures that could affect replacement cost, especially for which are used more heavily in commercial

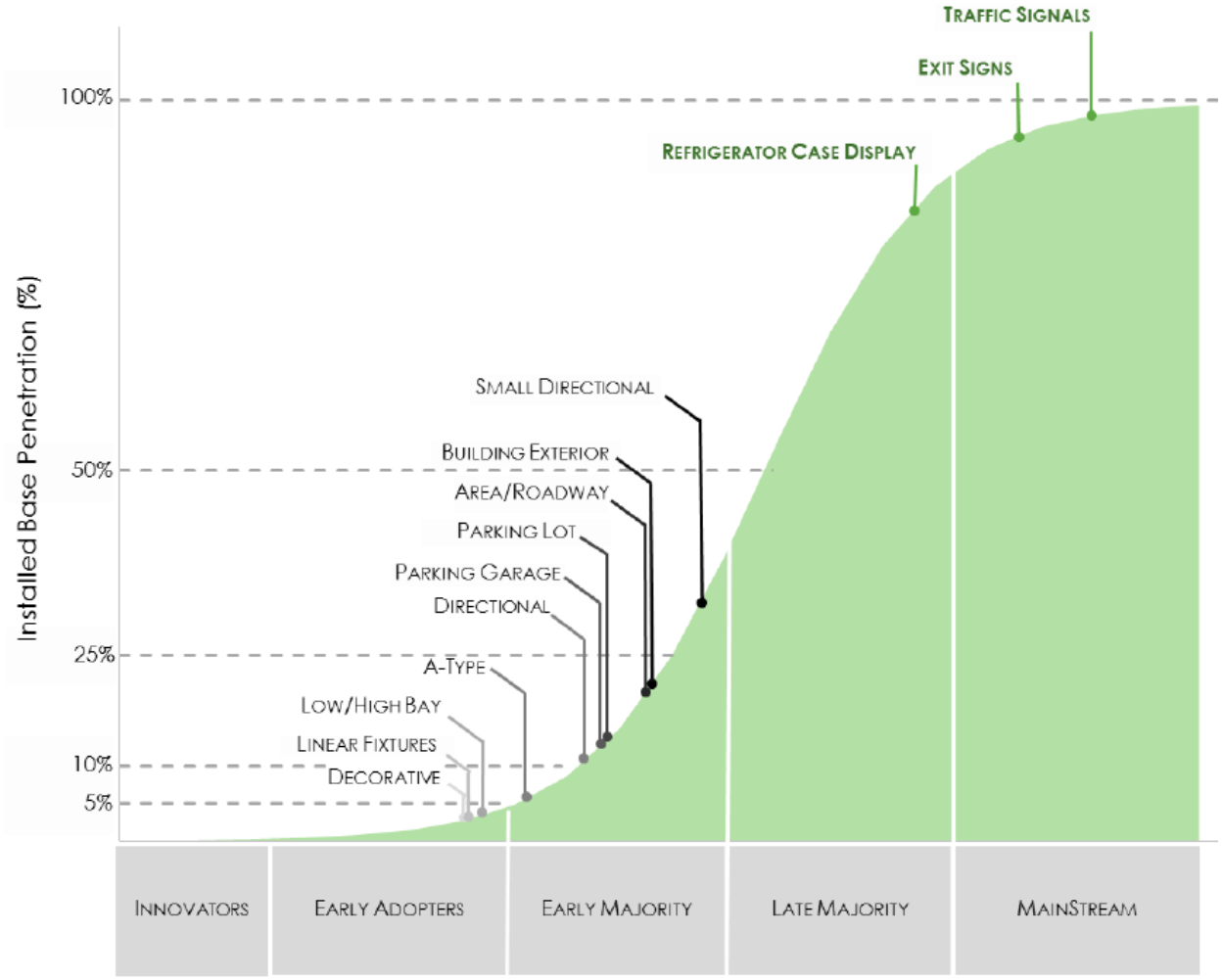

Figure 1.3. 2015 Penetration Rates of LED Lighting Applications

/ industrial applications with longer operating hours. The department of energy (DOE) expected that the replacement of light sources with LEDs by 2030 will dramatically reduce the energy consumption by 40 % with respect to the non-LED based light sources, and the DOE's scenario plans the power consumption by replacing LEDs to reduce additional 20 % more as shown in Figure 1.4 [6]. It is necessary to consider a way to reduce the replacement cost by utilizing the existing infrastructure system as well as the technology to maximize the

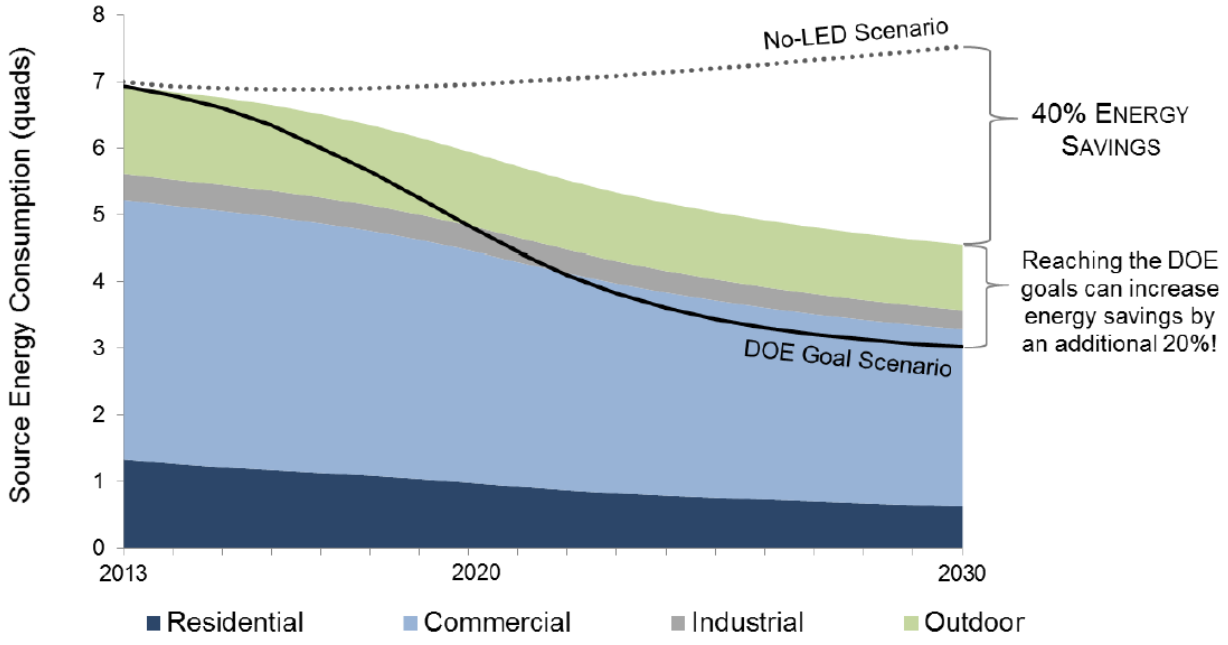

Figure 1.4. Forecasted U.S. Energy Savings if DOE SSL Program Goals are Realized

efficiency of the LED light source itself. In this dissertation, we have studied packaging materials and process optical properties that can improve the efficiency of LED emitter in general lightings, and presented packaging designs that can be applied to existing systems by only replacing the light source. In addition, we have also studied the LED-based backlights with color conversion films that can obtain a wider color gamut in display applications.

1.2. LED Packaging

The most significant improvement of the LED technology is that the efficiency is getting higher every year. This enhanced efficiency is mainly due to the extensive studies in recent years for the chip-level designs to reduce the effect called "efficiency droop", and the enhancement in light extraction efficiency using noble approaches such as chip-level reflectors, and optimizing chip geometry or surface morphology [7-10]. White LED is the most important light source in solid state lighting applications, which can dramatically reduce power consumption in general lightings. Figure 1.5 presents the plots of efficacy projection for the white LED packages. It has overcome 100 lm/W barriers already, and it is expected to breakthrough 200 lm/W by the year 2020 [11]. And the manufacturing cost for the LED emitter is expected to be reduced up to 20 % by 2020. As shown in Figure 1.6, the packaging cost is rapidly reduced compared to other components [12]. However, the efficacy droop by the packaging materials and process is estimated up to 20 % of overall performance, so there is a challenge for the packaging materials and process to enhance the efficacy in a limited budget. Therefore, the packaging components for the LED emitters are getting smaller and lighter, and the choice of materials used for LED packaging should be smarter to consider heat dissipation and light extraction with respect to the output power of

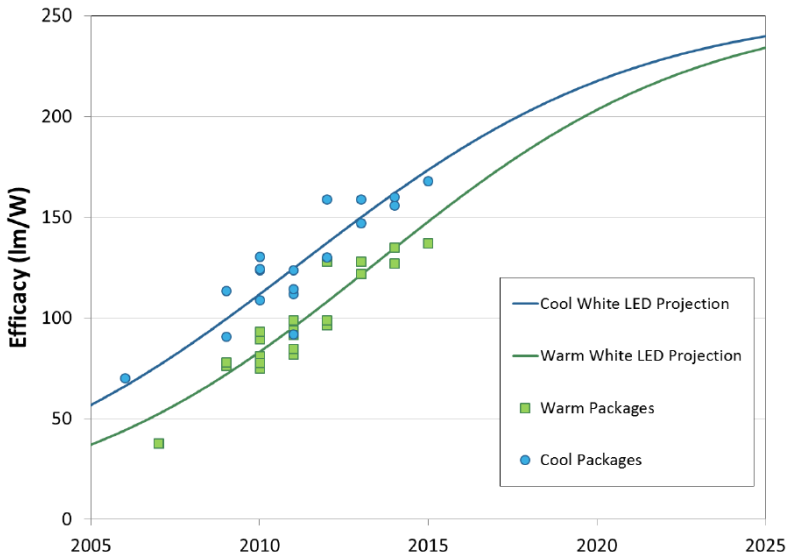

Figure 1.5. LED Package Efficacy Projections for Commercial Products

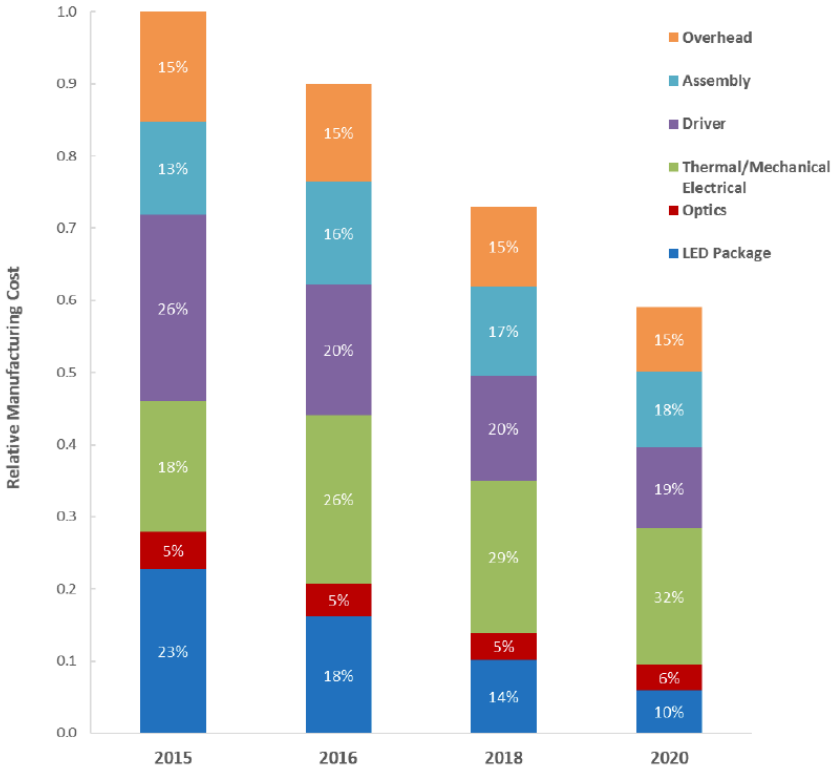

Figure 1.6. Cost Breakdown Projection for a Typical A19 Replacement Lamp

the LED die and driving circumstances for applications. Typically, high-power LEDs require much more complicated epitaxial process for the chip fabrication including multiple quantum well (MQW) with heterojunctions, and multi-layered noble chip level reflectors rather than mid-power LEDs as shown in Figure 1.7 [12, 13]. The junction temperature for the high-power LEDs should be much higher than mid power LEDs so that the package and fixture designs tend to be focused on better heat dissipation with the materials of higher thermal conductivity and the heat sinks in larger sizes [14]. On the other hand, the packaging

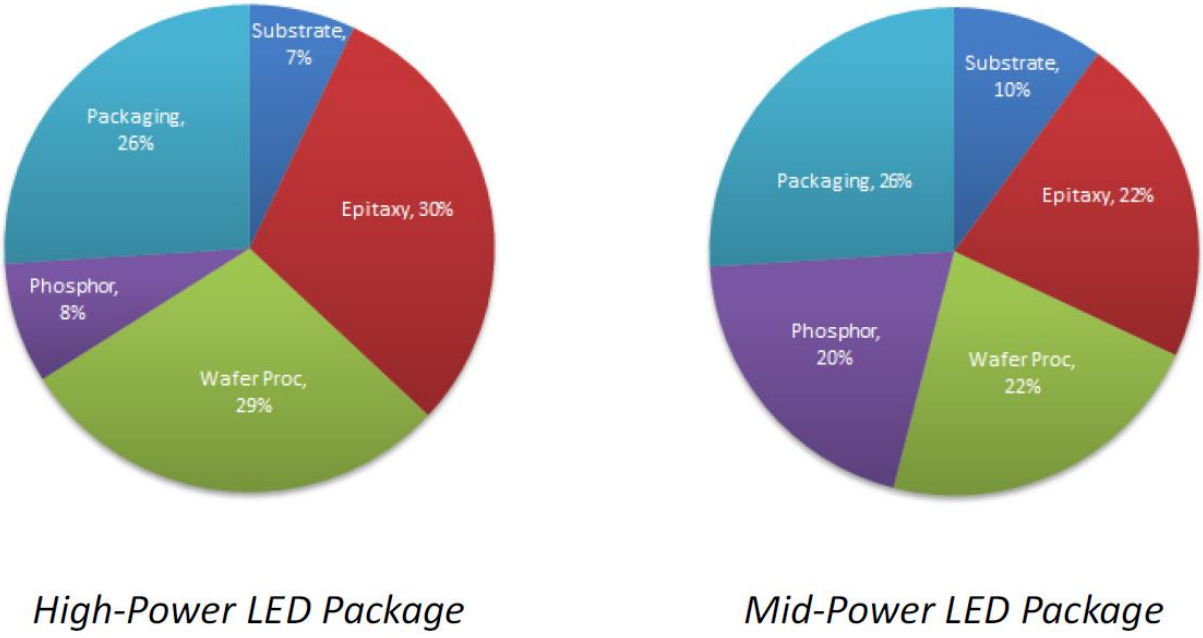

Figure 1.7. Typical Cost Breakdowns for High-Power and Mid-Power LED Packages

Figure 1.8. Examples of High-Power, Mid-Power, Chip-on-Board and Chip Scale LED Packages

materials for mid-power LEDs usually do not require complicated package designs or noble materials as shown in Figure 1.8, and therefore the fixture design could be simple and slim [11]. The backlight units for the high-end liquid crystal displays (LCDs) are almost made of mid-power LED emitters due to the simple and slim package designs. In addition, the consideration of optical property for LED packaging materials is crucial. Recent studies regarding packaging materials and process for the LEDs mainly focused on the thermal properties such as heat sink design, package substrate and die bonding materials with high thermal conductivity. For example, a typical die bonding material for the semiconductor packaging is an adhesive mixed with silver (Ag) particles, or a soldering paste in consideration of high thermal conductivity, and these types of die bonding materials have been directly used for LED packaging as well, as shown in Figure 1.9. The most crucial part is that the conventional die bonding materials are good for heat dissipation, but very poor in optical property, thus a substantial number of photons generated from the LED die is

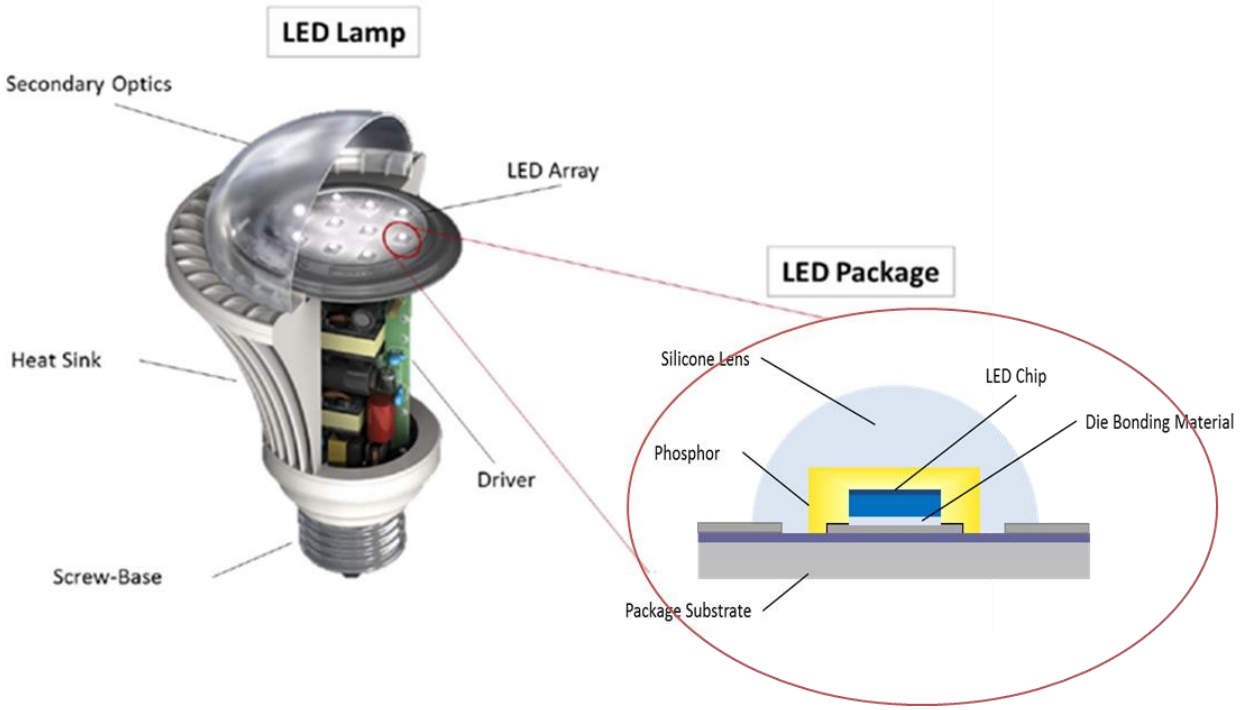

Figure 1.9. Components of an LED Lamp

Table 1.1. Present and Future Target Luminaire Efficiencies

Properties and effiacies of white light production and direction by luminaire, then of use by end user	Units	Present	Future (Targets)			
		2015	2018	2020	2025	Goal
Driver efficiency	%	0.88	0.91	0.93	0.95	0.95
Package efficacy (at 25°C)	lm/W	137	175	208	237	255
Thermal efficiency droop	%	0.88	0.91	0.93	0.95	0.95
Fixture (optical) efficiency	%	0.90	0.92	0.94	0.95	0.95
Luminaire Efficacy of White Light Production/Direction	lm/W	95	133	169	203	218

absorbed by the conventional die bonding materials. Thus, an adhesive material with a superior optical property and a decent thermal conductivity is required to replace conventional die bonding materials. Current optical efficiency for a white LED luminaire presented in Table 1.1 is 90 %, and this is almost the same as thermal efficiency of 88 % [11].

1.3. WIDE COLOR GAMUT (WCG) DISPLAYS

Liquid crystal display (LCD) backlighting is the largest market for the mid-power LEDs applications even though the demand on general lightings applications is rapidly chasing it. Most of the LCDs use white backlights, and the white light source is filtered by the red, green, and blue color filters at the end of the display to obtain a color display. The schematic cross-sectional view is illustrated in Figure 1.10. The backlight unit is the most important component for the LCDs in terms of the power consumption, hence the conventional white LEDs (WLEDs) using YAG:Ce-based phosphors on the blue LEDs are well known as the highest power conversion efficiency have long been used for the LCD backlights to obtain a white light. However, the YAG-WLED is not a good light source for the LCD backlights although its high efficiency because of the existence of the color filters. The YAG-WLED has a broad yellow peak to obtain white emission, and a substantial amount of the yellow emission is blocked and wasted by the red and green color filters as shown in Figure 1.11a [15]. Moreover, the FWHM of each red and green emission filtered is dependent on the FWHM of each color filter, so that the color quality of resulted red and green emission is less saturated. The color standard for HDTVs used to be Rec. 709 as shown in Figure 1.12, and conventional YAG-WLED met that standard. However, due to the demand of wide color

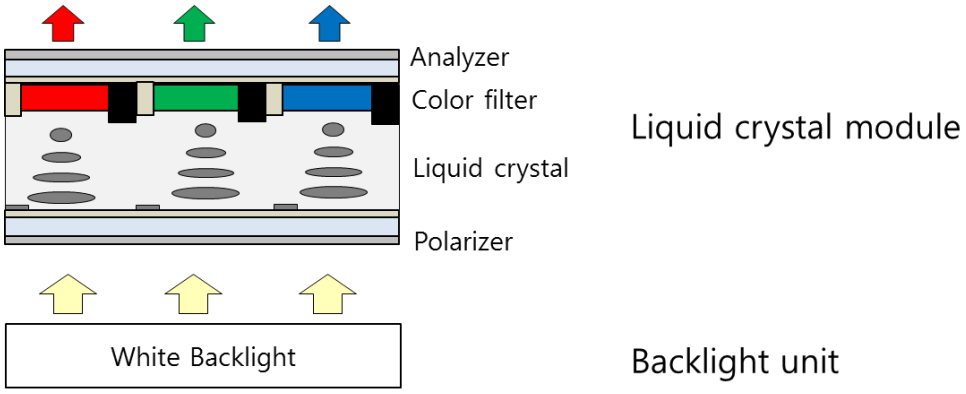

Figure 1.10. Schematic cross-sectional view of a typical LCD display

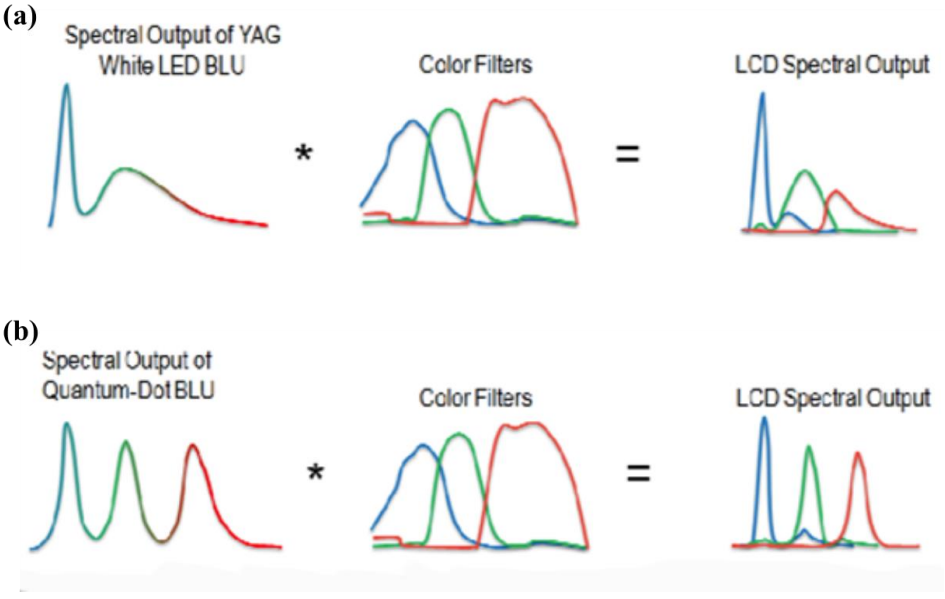

Figure 1.11. Backlight color interaction with color filters for (a) conventional YAG-WLED and (b) Quantum-dot based LED

gamut (WCG) displays, the innovative mobile displays are required to meet DCI-P3 standard, and the Rec. 2020 standard is strongly recommended for upcoming UHDTVs. Hence, much more saturated red and green emission from the backlight is required to obtain a WCG display. A backlight unit using red/green/blue LEDs has been introduced to obtain a WCG display, however this method was not cost-effective because the manufacturing cost is much

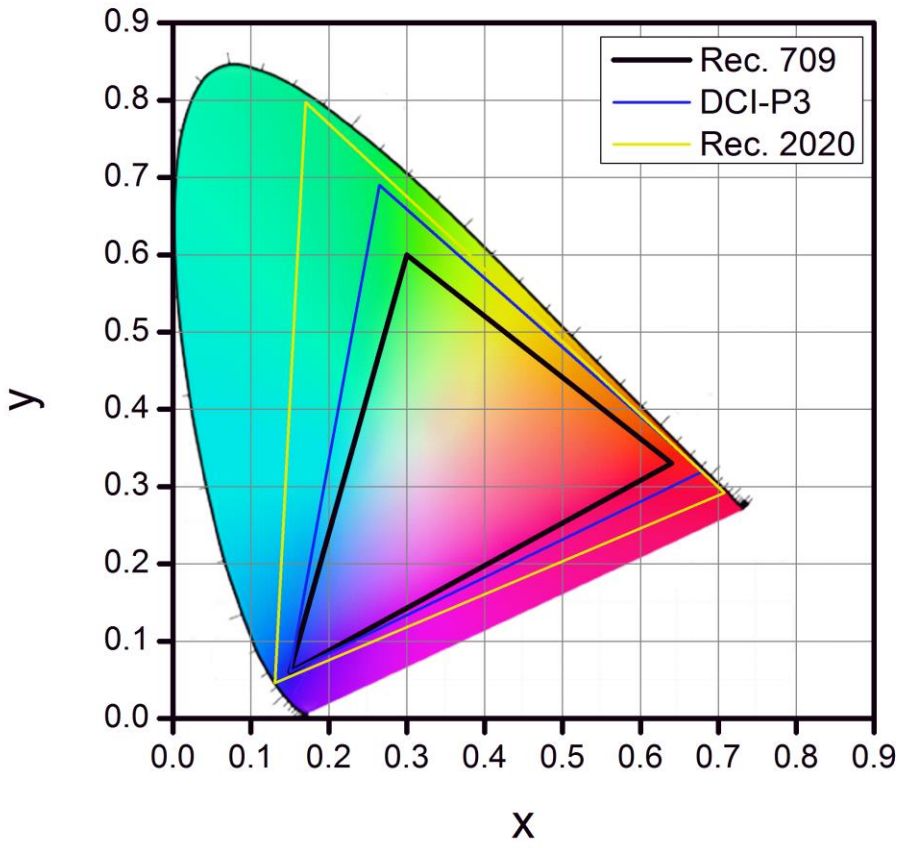

Figure 1.12. CIE 1931 color gamut for Rec. 709, DCI-P3, and Rec. 2020

higher than YAG-WLED based backlight unit due to the increased amount of driving circuits and the long-term reliability issue in white balance.

Quantum dots (QDs) are nanometer-sized semiconductor materials which exhibit quantum confinement effects. QDs are usually synthesized as core-shell structures of compound semiconductor materials to enhance quantum efficiency and reliability, and ligands are usually attached to the outer surface of the QD as shown in Figure 1.13. The inorganic core is surrounded by the inorganic shell, which is in turn passivated by organic

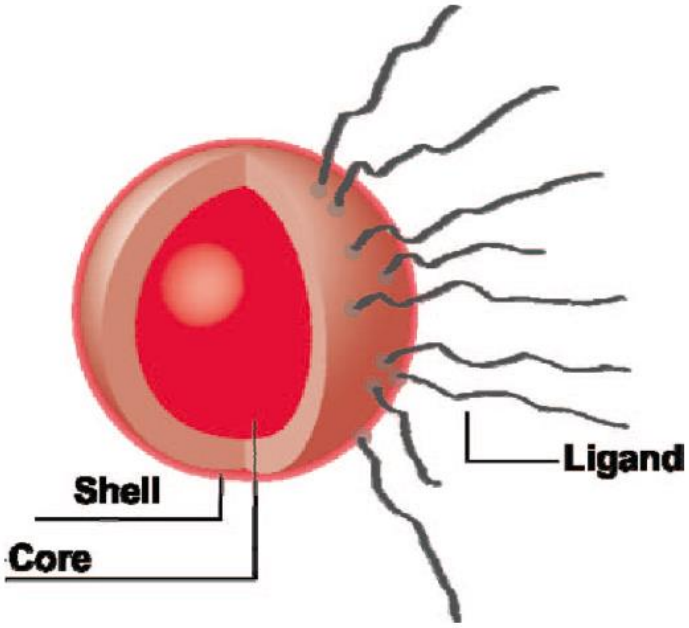

Figure 1.13. Graphical depiction of a core-shell quantum dot with surrounding ligands.

ligands that allow the material to be processed as a liquid suspension. When the QDs are irradiated by light from an excitation source to reach energy excitation states, they emit energies corresponding to the respective energy band gaps. Since the control over the size of the QDs effectively controls the corresponding band gaps, energies of various wavelength regions can be obtained [16]. In other words, replacement of conventional phosphors with well controlled size of the QD particles as photoluminescent materials ensure to match wavelength bands with each color filter, as well as to narrow down FWHM for the emission with uniform particle distribution, which is desired for WCG displays as shown in Figure 1.11b [17, 18]. Extensive studies have been proceeded, and several different implementation geometries using QDs for color conversion sources are contemplated as shown in Figure 1.14 [19]. A) On-chip, where the QDs are directly replaced conventional phosphors within the LED package which is coupled to the light guide, is one of the earliest stages. This structure is directly applicable to the existing manufacturing process, less modification in fabrication is required. However, QD materials easily loss quantum efficiency under exposure of moisture and heat, the encapsulation materials such as epoxy or silicone are not sufficient for passivation from the moisture, and the blue LED chip which is the heat source for the QDs is too close. B) On-edge, where the QDs are placed in between the LED package and the light guide plate by packaging within a glass rod, is more advanced structure by taking advantage of passivation from moisture and heat. This is only applicable for edge-lit type backlights. C) On-surface, called as QDEF, where the QDs are in a thin film over the entire display area [20]. This can be applicable for either edge-lit or direct type backlight, but the amount of QDs required is dramatically increased proportional to the screen size, and therefore not cost-effective for the displays in large sizes because the QD materials are much more expensive

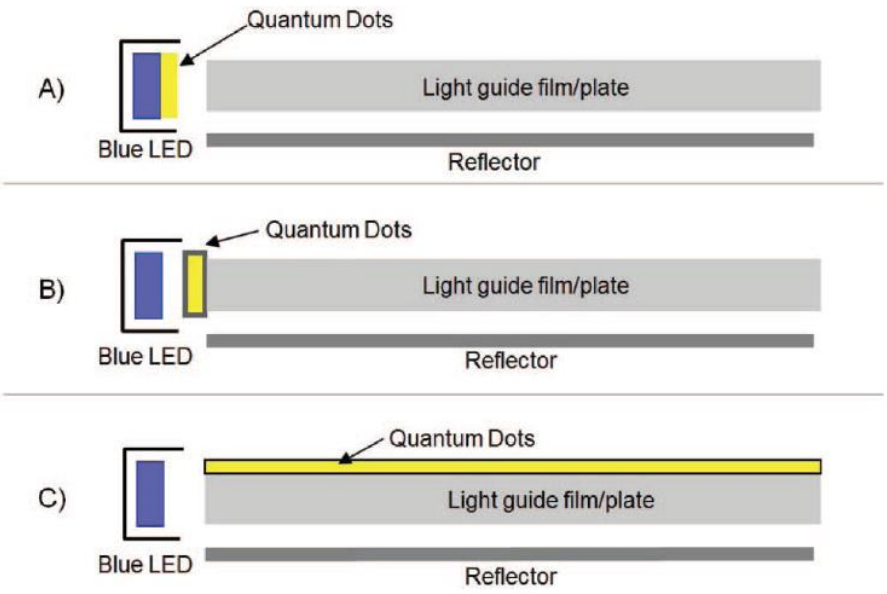

Figure 1.14. Depiction of the three different implementation geometries contemplated. A) On-chip, B) On-edge, and C) On-surface

than YAG-based phosphors. Thus, each packaging design is confronted important problems to solve, and this dissertation is focused on reducing amount of QD materials while maintaining an equivalent optical performance for the WCG display.

REFERENCES

[1] E. F. Schubert, T. Gessmann, and J. K. Kim, "Light Emitting Diodes," *Kirk-Othmer Encyclopedia of Chemical Technology*: John Wiley & Sons, Inc., 2000.

[2] S. Pimputkar, J. S. Speck, S. P. DenBaars *et al.*, "Prospects for LED lighting," *Nat Photon,* vol. 3, no. 4, pp. 180-182, 2009.

[3] S. Nakamura, and M. R. Krames, "History of Gallium-Nitride-Based Light-Emitting Diodes for Illumination," *Proceedings of the IEEE,* vol. 101, no. 10, pp. 2211-2220, 2013.

[4] "Adoption Analysis," *DOE SSL Program*, 2016.

[5] W. Rhodes, and IHS, *Smart Lighting Conference, Berlin*, 2015.

[6] "Energy Savings Forecast of Solid-State Lighting in General Illumination Applications," *DOE SSL Program*, 2014.

[7] Y. P. Hsu, S. J. Chang, Y. K. Su *et al.*, "InGaN/GaN light-emitting diodes with a reflector at the backside of sapphire substrates," *Journal of Electronic Materials,* vol. 32, no. 5, pp. 403-406, 2003/05/01, 2003.

[8] J. K. Kim, J. Q. Xi, and E. F. Schubert, "Omni-directional reflectors for light-emitting diodes." pp. 61340D-61340D-12.

[9] J. Q. Xi, H. Luo, A. J. Pasquale *et al.*, "Enhanced Light Extraction in GaInN Light-Emitting Diode With Pyramid Reflector," *Photonics Technology Letters, IEEE,* vol. 18, no. 22, pp. 2347-2349, 2006.

[10] N. M. Lin, S. Shei, and S. Chang, "Nitride-Based LEDs With High-Reflectance and Wide-Angle Ag Mirror + SiO2 /TiO2 DBR Backside Reflector," *Lightwave Technology, Journal of,* vol. 29, no. 7, pp. 1033-1038, 2011.

[11] "R&D Plan," *DOE SSL Program*, 2016.

[12] "Inputs from DOE SSL Roundtable and Workshop attendees."

[13] Y. Bohan, Y. Jiun-Pyng, N. T. Tran *et al.*, "Influence of Die Attach Layer on Thermal Performance of High Power Light Emitting Diodes," *Components and Packaging Technologies, IEEE Transactions on,* vol. 33, no. 4, pp. 722-727, 2010.

[14] M.-H. Chang, D. Das, and M. Pecht, "Junction Temperature Characterization of High Power Light Emitting Diodes." pp. 23-24.

[15] J. V. Derlofske, G. Benoit, A. Lathrop *et al.*, "Quantum Dot Enhancement of Color for LCD Systems," *3M Company*, 2013.

[16] G.-W. Kim, J.-B. Park, D.-C. Cho *et al.*, "Light emitting diode, backlight assembly having the same and method thereof," US7819539 B2, U.S. Patents, 2010.

[17] A. Lathrop, "Color as a Key Differentiator," *IHS/SID 2013 Business Conference*, 2013.

[18] J. Chen, V. Hardev, J. Hartlove *et al.*, "A High-Efficiency Wide-Color-Gamut Solid-State Backlight System for LCDs Using Quantum Dot Enhancement Film," *SID Symposium Digest of Technical Papers,* vol. 43, no. 1, pp. 895-896, 2012.

[19] S. Coe-Sullivan, W. Liu, P. Allen *et al.*, "Quantum dots for LED downconversion in display applications," *ECS Journal of Solid State Science and Technology,* vol. 2, no. 2, pp. R3026-R3030, 2013.

[20] J. V. Derlofske, J. Schumacher, J. Hillis *et al.*, "Quantum Dot Enhancement Film (QDEF)," *3M White Paper*, 2013.

CHAPTER 2

OPTICAL ROLE OF DIE ATTACH ADHESIVE FOR WHITE LED EMITTERS: LIGHT OUTPUT ENHANCEMENT WITHOUT CHIP-LEVEL REFLECTORS

2.1. INTRODUCTION

The Gallium nitride (GaN) based mid-power (input current less than 350 mA and input power less than 0.8 W) mesa type light emitting diodes (LEDs) dominate the current LED lighting and backlighting applications because of their cost effectiveness as well as relatively high performance [1-3]. For those LEDs, various types of chip-level backside reflectors (BRs) with a reflectance as high as of 98% have been developed for adding on their backside, with an aim of enhancing its light output. An enhancement of as high as of 50 % is reported [4-6]. Because of those results, the chip level BR is now often adopted as a part of mesa-LED chip structure. However, the reported enhancement measurements based on the naked chip [4, 5] might not be relevant to practical applications: Firstly, an enhancement from a naked chip does not necessarily lead to an equivalent enhancement for a packaged LED emitter. This is because light output of the LED emitter is strongly influenced by packaging materials and process [7, 8]. Secondly, not every BR achieves the highest reflectivity, but Au-based reflective layer has been typically used for low cost LED chips despite relatively lower reflectivity at the wavelength shorter than 550 nm. The introduction of BRs is also historically related to the conventional silver-based die attach adhesive (DAA)

which is optically absorptive and thus a highly optically reflective BR can reduce the absorption of downward photoemission from the multiple quantum well (MQW). Over last few years, however, an optically clear DAA (CDAA) has been introduced, which can have significant impact on the role of BRs for mesa type LEDs [9].

Hence, the objective of the present work is to investigate light output difference from a packaged LED emitter using a BR-free and BR-based chip as a function of packaging materials and processes, by using Monte Carlo simulations. Contrary to prior reports based on naked chips, it is demonstrated for the first time that the light output of a packaged LED emitter with a BR-free chip can indeed be as high as that of the emitter using the same chip but with an added backside reflector when the optically clear DAA replacing conventional silver type DAA and a few other key packaging materials and processes are optimized.

2.2. APPROACH

A schematic cross-sectional drawing of a packaged blue LED emitter is shown in Figure 2.1(a), and the corresponding optical model for the Monte Carlo simulation using *LightTools* is illustrated in Figure 2.1(b). The thickness of each layer and its respective relative refractive index [5] can be found in Figure 2.1(c). In case of the BR-based LED chips, a metal reflector layer of 150 nm is added on the bottom of the chip. For the optical simulation, 2 million rays are traced and the simulation error to be maintained less than 1 % for each simulation run. An input current of 120 mA is used and the chip (24 ×24 mil in size) has a dominant wavelength of 450 nm. Absorption coefficients for the GaN and the MQW are 200 cm-1 and 3600 cm-1, respectively [10, 11]. For the BR-based chip, commercially available LED chips with two different BR materials are selected: the BR with

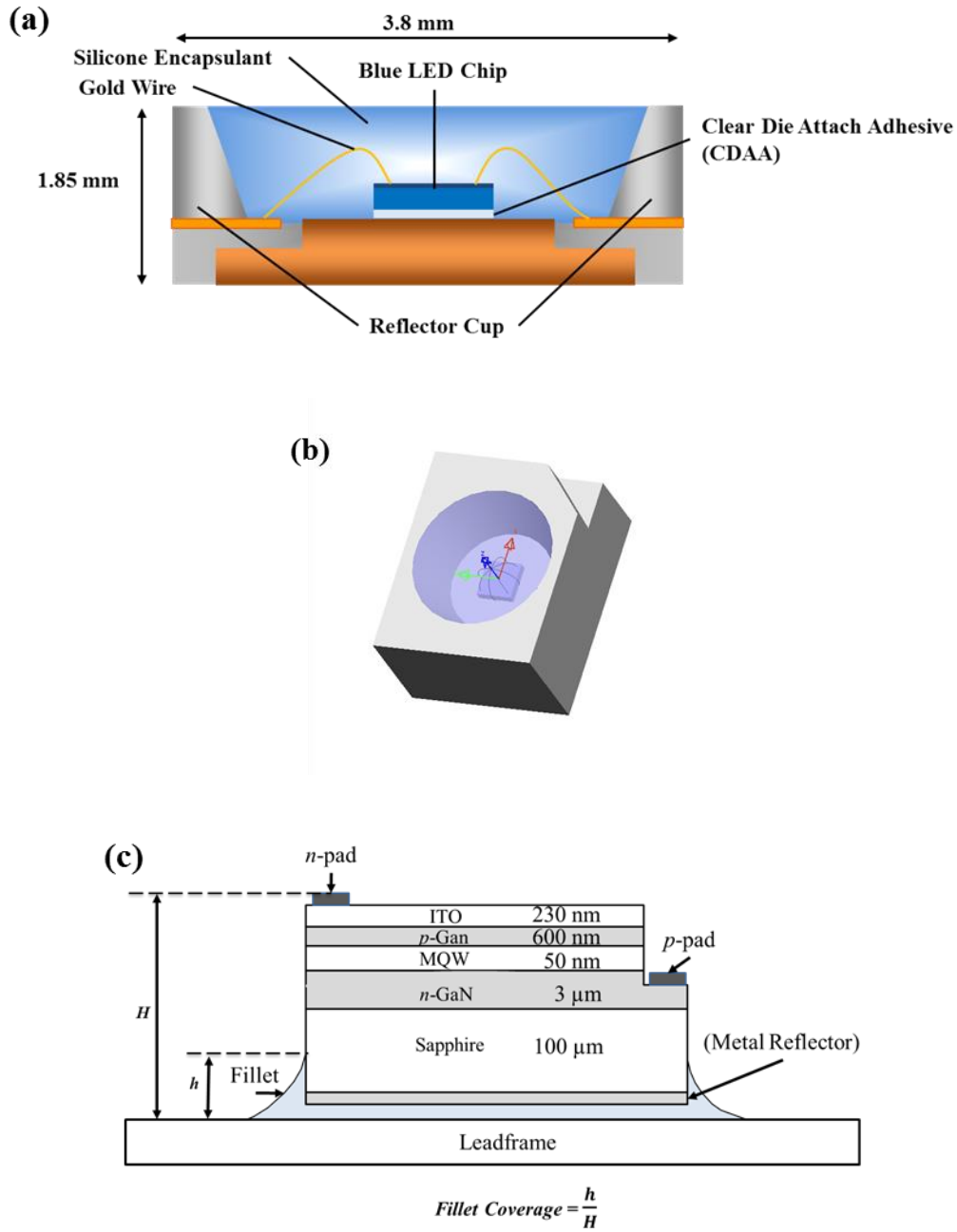

Figure 2.1. Leadframe based LED emitter. (a) Schematic cross section of a packaged LED emitter by using optically clear die attach adhesive (CDAA), (b) optical model used in Monte-Carlo simulations and (c) microscopic enlargement of the blue LED chip attached on the leadframe substrate by using CDAA. Layers are not plotted in their relative thickness in order to present illustration. The size of the chip is 24 × 24 mil (0.61 × 0.61 mm) and the thickness is about 100 µm.

the reflectivity of 98 % at 450 nm by consisting of 3-layers of DBR (Distributed Bragg Reflector) and Ag plating, and the Au-based BR [12]. Due to the metal plating for each BR, the transmission through the BR is not considered and therefore the light output which is not reflected at the interface is absorbed during the simulations. The package has the dimension of 3.5 × 2.8 × 1.85 mm, the depth of the diffusively reflective cup (with a reflectance of 95 %) is 0.9 mm, and its upper and lower diameters are 2.4 mm and 1.75 mm, respectively. The reflectance for the leadframe substrate (R_{LF}) ranges from 80 % to 99 % [13]. For the experimental samples, three groups of leadframe substrates with different reflectance are employed. The measured reflectance for each group is presented in Table 2.1. The silicone encapsulant has a relative refractive index of 1.53, and the optical transmittance for 1 mm in thickness is 99 %, all at the wavelength of 450 nm [14]. For WLED emitters used in this work, 7.5 wt. % of yellow phosphor powder with dominant peak wavelength of 535 nm is distributed by mixing with the encapsulant [15] and resulted correlated color temperature (CCT) is 9,000 K.

Table 2.1. Reflectance for Leadframe Substrates

Index	A	B	C
Reflectance* (%)	82.1	88.2	94.2

*Reflectance at the wavelength of 450 nm.

Two types of DAA materials are used for die bonding. One is an optically clear DAA (CDAA) formulated by Shi group [16] and the other is commercially available conventional silver-epoxy based DAA (denoted as AgDAA). For the CDAA, optical transmittance is set of 85 % for 1 mm in thickness, and the relative refractive index is ranging from 1.42 to 1.78. For the packaging parameters of the CDAA, the range of the bondline thickness is from 5 μm to 25 μm [17]. The fillet coverage by CDAA is set up to 40 % of the chip height for the experimental measurement.

The junction temperature which affects luminous efficiency for the LED emitter is proportional to input current, thus thermal management in high-power LEDs has been widely considered [7, 18]. However, the possible thermal-radiation coupling is not considered in the simulations because relatively lower power is involved in the present case of mid-power LEDs [19].

The packaging process for experimental measurement is as follows: (1) the leadframe with same dimensions described above is cleaned by isopropyl alcohol and baked at 80 °C before used; (2) a blue LED chip is attached to the center of the leadframe substrate by using CDAA, and different bonding forces are applied to obtain different bondline thickness; (3) the samples are then cured at 150 °C for 2 hours; (4) wire-bonding is performed for interconnect between the LED chip and the leadframe; (5) silicone encapsulant is injected into the reflective cup; (6) the samples then are cured at 150 °C for 2 hours; (7) The packaged LED emitters are then soldered to Al-based printed circuit board (PCB). Everfine power generator with constant current mode of 120 mA is used. Light output of packaged LED emitters is measured in a LabSphere integrating sphere.

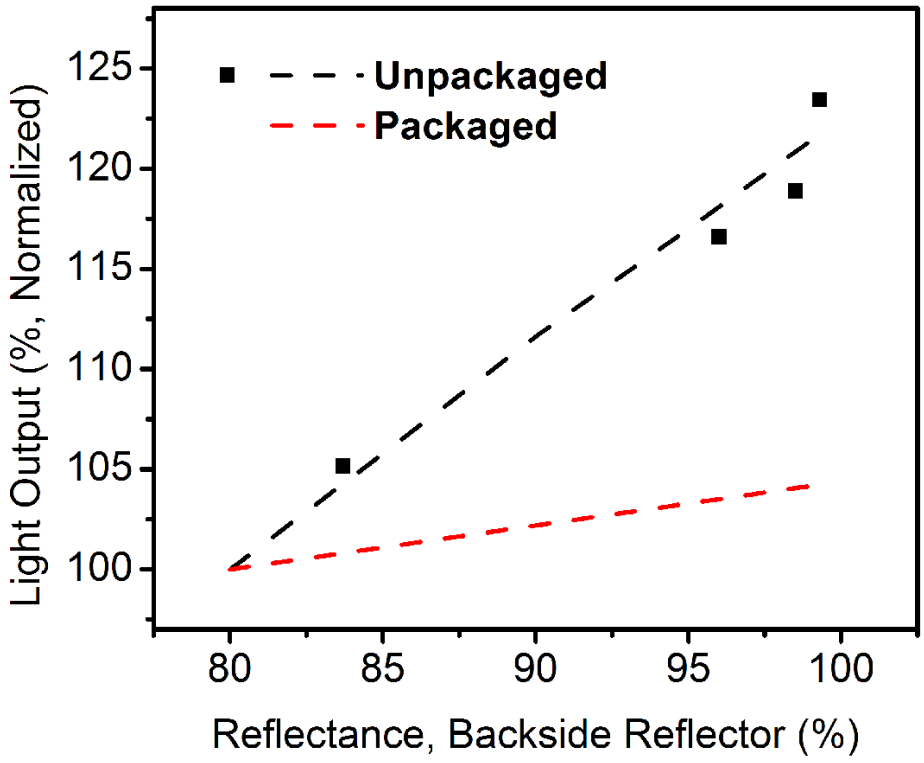

Figure 2.2. Naked chip vs. Packaged emitter; Light output for unpackaged naked blue LEDs and packaged blue LED emitters as a function of reflectance for the backside reflector (R_{BR}).

For the verification of the current simulations, the simulated results for the light output as a function of BR reflectance (R_{BR}) for the naked monotonic blue color emitting LED chip, are compared with the available experimental data [5]. As shown in Figure 2.2, it is evident the simulation is fully supported by the experimental observation, which provides the tangential support for the simulation method adopted in the present work. It is interesting to note a strong difference between the naked LED chip and packaged LED emitter in terms of the light out dependence on R_{BR}: Due to the influence by the packaging materials and parameters, the enhancement by the BR in light output of the packaged emitter is not as much as for the naked chip, which suggests a possible diminished role of BR in enhancing the light output for a packaged emitter, demonstrated as follows.

The light output of packaged LED emitter as a function of fillet coverage is also shown in Figure 2.3. Due to much lower photo absorption by the CDAA compared to the conventional AgDAA, the light output is not reduced up to 40% of CDAA fillet coverage. The comparison of light output between BR-based and BR-free LED emitter is done by using CDAA.

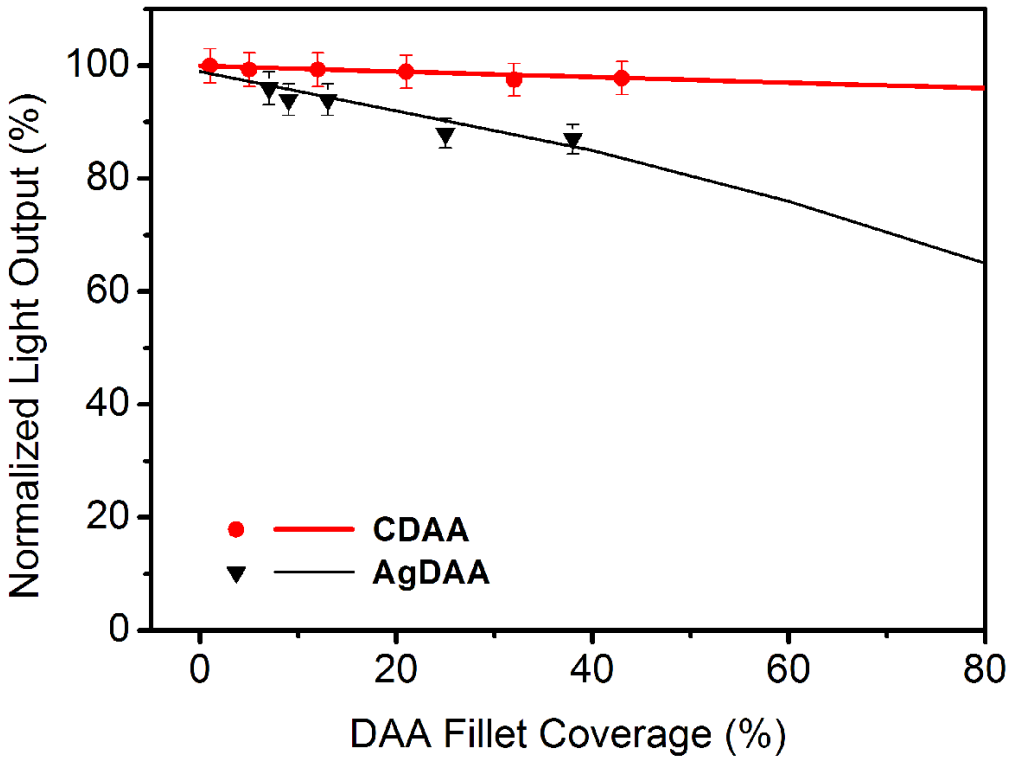

Figure 2.3. CDAA vs. AgDAA. Light output of blue LED emitters encapsulated with silicone encapsulant as a function of DAA fillet coverage. The Optically clear DAA is denoted as CDAA and the conventional DAA with silver paste is denoted as AgDAA. Error estimated for the simulation is 0.944 %.

2.3. RESULT AND DISCUSSION

2.3.1. Light Output of Packaged LED Emitters vs Reflectance of Leadframe Substrate

Figure 2.4 presents the light output of blue and white LED emitters as a function of the reflectance of leadframe substrate, R_{LF}. The bondline thickness of the CDAA is 5 μm, which is typical in applications. The results show that BR-free emitter exhibits much higher light output than Au-BR based emitter while the BR-based emitter with R_{BR} is 98 % as an extreme case shows the highest light output. Note that current BR materials used in industry are still Au-based in general, especially for mid-power and low-cost chips. Due to the absorption of Au based BR for the wavelength of shorter than 550 nm [12], light output for the Au BR based emitter is much lower than BR-free emitters performed in both simulations and experimental measurements. Although the role of the BR with R_{BR} of 98 % which contributes to the light output enhancement can be still found, the enhancement due to the BR for the BR-based blue LED and WLED emitters diminish to only 6 % and 7 %, respectively. It is much weaker than the reported naked chip level enhancement, and even more diminished when the R_{LF} is getting increased. Unlike the conventional LED packaging by using silver based DAA, substantial amount of photo absorption by the DAA can be avoided by adopting CDAA. Thus, the BR might not be necessary when the R_{LF} reaches to an optimized reflectance due to the diminished role of the BR at relatively higher R_{LF}. In addition, a removal of the BR allows LED chips having much simpler structure than BR-based chips. This approach may lead to a cost reduction of about 5 to 10% for chip fabrication not only by reduced number of process and materials, but also by improved uniformity in optical characteristics due to those simple structure and fabrication process. Hence, LED emitters

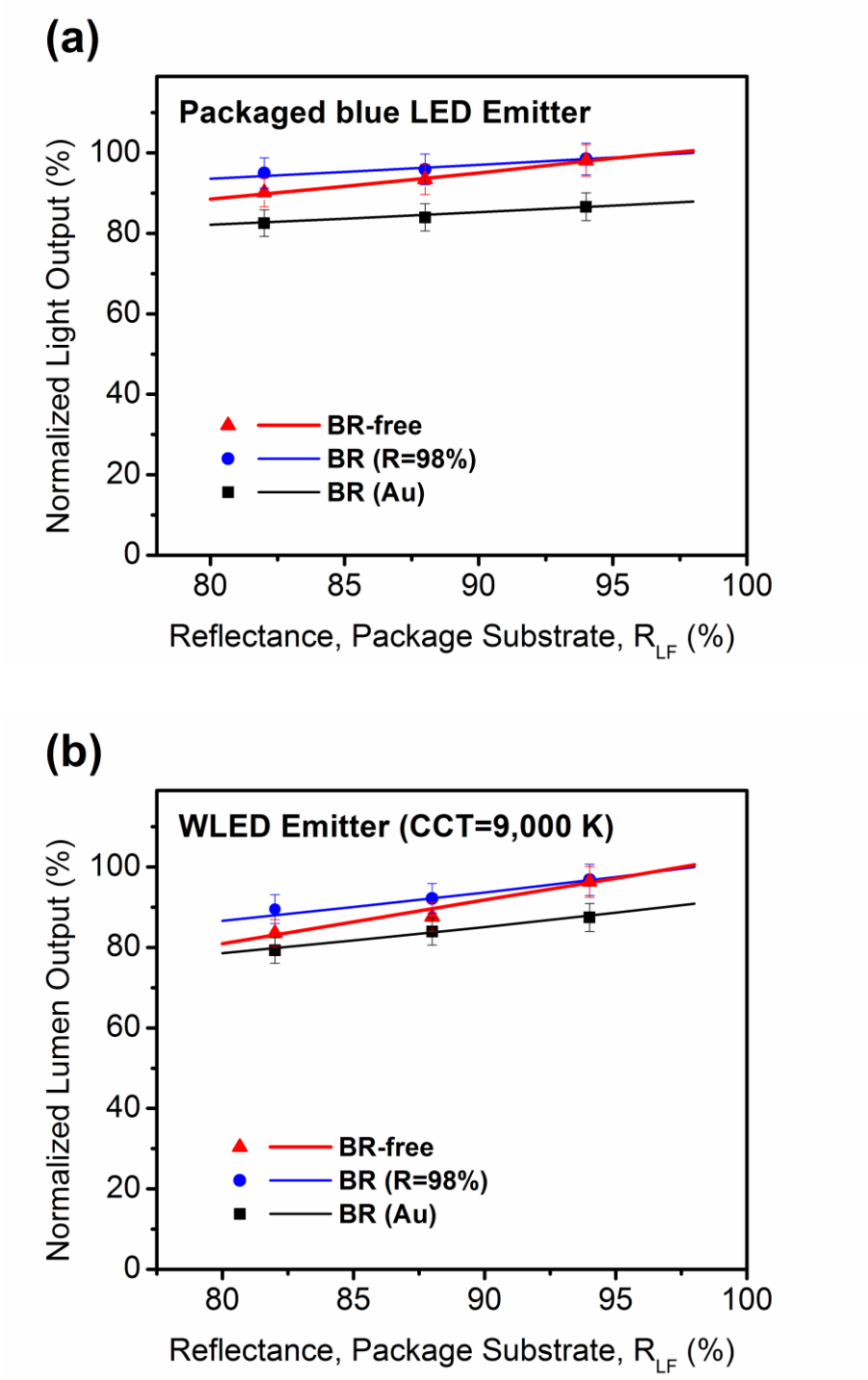

Figure 2.4. Light output of BR-free emitters; Light output of (a) a blue LED and (b) a white LED emitters with BR-based and BR-free chip as a function of reflectance of the leadframe substrate (R_{LF}). Bondline thickness of the CDAA is 5 µm. Results are normalized by the light output of BR (R_{BR} = 98 %) based emitter at R_{LF} of 98 %. Error estimated for the simulation is 0.814 %.

with simple BR-free chips may further improve performance to cost ratio for manufacturing LED applications.

The light output for the BR-free emitter is more dependent on the R_{LF} than the BR-based emitter because the portion of reflected photons by leadframe substrate is greater due to optically transparent interface between the LED chip and CDAA. Hence, it is evident that the R_{LF} is a dominant parameter to obtain higher light output, and therefore higher reflectance for the leadframe substrate is preferred for enhancing optical performance of LED emitters.

2.3.2. Light Output of Packaged LED Emitters vs Thickness of CDAA

The light output of blue LED emitters and WLED emitters as a function of CDAA bondline thickness are shown in Figure 2.5. A light output enhancement is observed in case of a BR-free emitter, by optimized refractive index of 1.53 for the CDAA, as shown in Figure 2.5(a). The results show that increased bondline thickness from 5 μm to 25 μm further enhances light output for the BR-free emitters up to 2 % while the BR-based emitters maintain the difference of the light output within 0.1 %. The light output for the Au-BR based emitter is still much lower than BR-free emitters due to the absorption less than 550 nm. Figure 2.5(b) presents the luminous output of white LED emitters by using CDAA with the refractive index of 1.53. The light output of the BR-free emitter is more enhanced by increased bondline thickness of the CDAA for both blue and white LEDs.

The R_{LF} is a dominant parameter for a BR-free emitter to enhance light output as we discussed above. And the optimization of optical properties and process parameters for the CDAA besides the R_{LF} would be also an important factor due to the reasons as follows: Firstly,

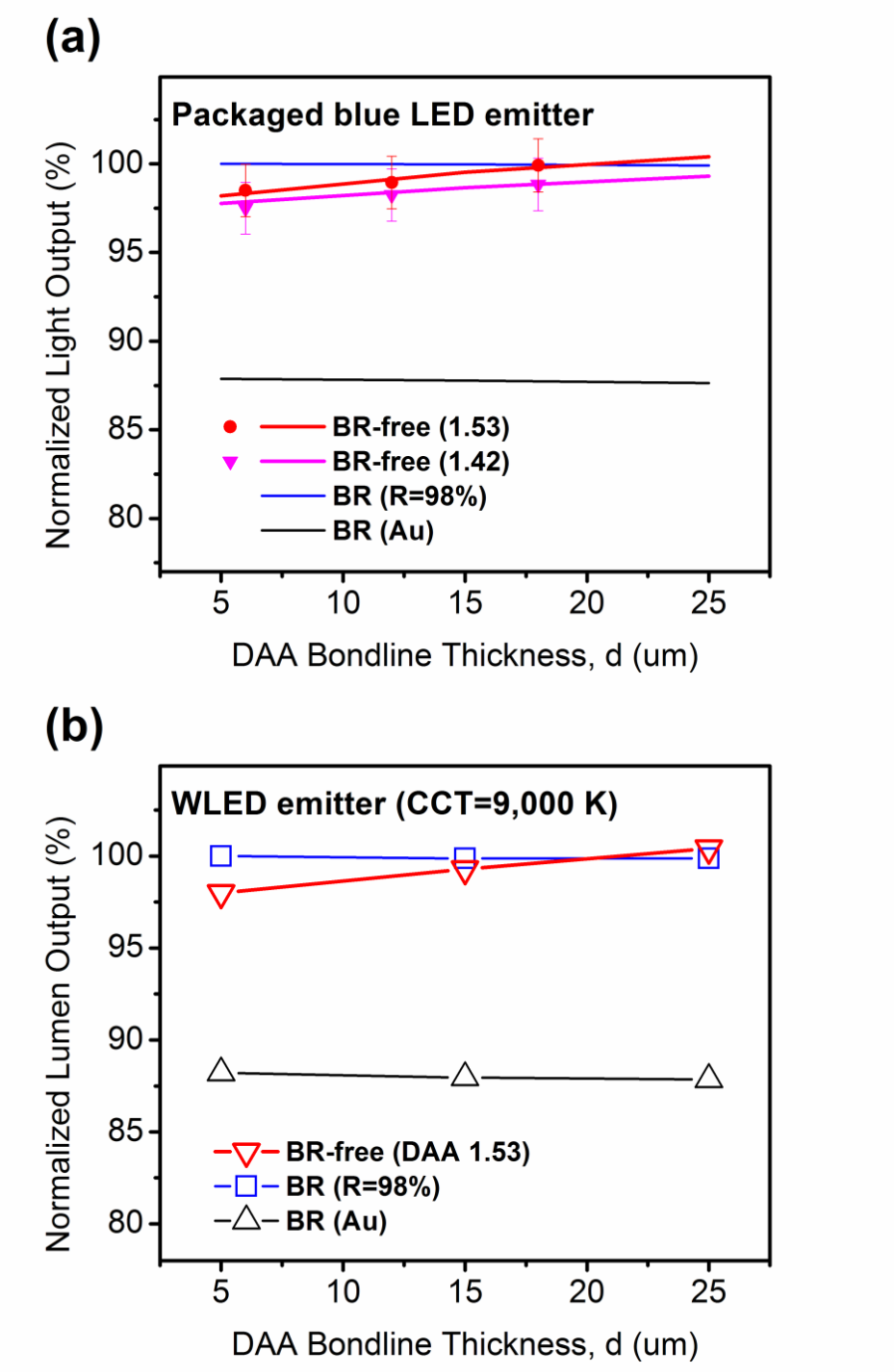

Figure 2.5. Light output by CDAA; Light output of (a) blue LED emitters with different refractive indices for CDAA and (b) simulation of the white LED emitter as a function of CDAA bondline thickness, d. Reflectance for the leadframe substrate (R_{LF}) is 88.2 %. Results are normalized by the light output of BR (R_{BR} = 98%) based emitter at d of 5 μm. Error estimated for the simulation is 0.917 %.

a higher reflectance may require surface treatment on the leadframe substrate [20], which causes an increase in manufacturing cost. Secondly, it is still challenging that the leadframe substrate obtains such higher reflectance because there exists an upper limit of reflectance for the metal plating in practical applications [21]. An enhancement in light output for the BR-free emitter is observed by using an optimized relative refractive index of 1.53 for the CDAA, which is a matched refractive index with the encapsulant. This allows a part of downward photoemission reflected by the leadframe substrate not being trapped by CDAA and re-absorbed by GaN-based active layers, but being extracted towards encapsulation region through the interface between CDAA and encapsulant, and thus contributes to enhancement in light output. That interface is more expanded by increased bondline thickness, and therefore the light output for the BR-free emitter is much further enhanced with relatively low R_{LF} with respect to the BR with the R_{BR} of 98 %. The enhancement of 2 % by optimized process parameters for the CDAA is within the experimental error. However, the tendency of light output enhancement has shown that the simulation results are remarkable.

In addition, increased bondline thickness of the CDAA also affects the thermal resistance of the DAA region due to lower thermal conductivity of the CDAA compared to conventional DAA materials [16]. This optimization process is thus only preferable for low to mid-power LED applications (input current less than 350 mA) because junction temperature control by heat dissipation is much more crucial for such high-power LED applications in order to maintain optical performances.

2.4. CONCLUSIONS

In this study, key packaging material and process parameters for the packaged LED emitter in order to enhance light output were determined. The actual contribution of chip-level BRs to light output by two different types of BRs, and the practical role of optically transparent DAA, optimized packaging materials and process parameters were investigated at the packaged LED emitter level. Monte Carlo simulations were conducted to estimate optimal packaging parameters in light output. The results suggest that the influence of optimized packaging material and process parameters on light output is more dominant for LED emitters rather than previously reported effect by the chip-level BRs, and a simple-structured and cost-effective BR-free LED chip is able to achieve an equivalent light output to a conventional BR-based chip by packaging with optimized dominant parameters.

REFERENCES

[1] Huang, H. W., Lin, C. H., Yu, C. C., Lee, B. D., Chiu, C. H., Lai, C. F., Kuo, H. C., Leung, K. M., Lu, T. C., and Wang, S. C. Enhanced light output from a nitride-based power chip of green light-emitting diodes with nano-rough surface using nanoimprint lithography. Nanotechnology, 2008; 19(18), 185301.

[2] Masui, H., Yamada, H., Iso, K., Speck, J. S., Nakamura, S., and DenBaars, S. P. Non-polar-oriented InGaN light-emitting diodes for liquid-crystal-display backlighting. Journal of the Society for Information Display, 2008; 16(4), 571-578.

[3] Lee, C.-L., Lee, S.-C., and Lee, W.-I. Nonlithographic Random Masking and Regrowth of GaN Microhillocks to Improve Light-Emitting Diode Efficiency. Japanese Journal of Applied Physics, 2006; 45(1L), L4.

[4] Chen, H., Guo, H., Zhang, P., Zhang, X., Liu, H., Wang, S., and Cui, Y. Enhanced Performance of GaN-Based Light-Emitting Diodes by Using Al Mirror and Atomic Layer Deposition-TiO2 /Al2O3 Distributed Bragg Reflector Backside Reflector with Patterned Sapphire Substrate. Applied Physics Express, 2013; 6(2), 022101.

[5] Lin, N. M., Shei, S., and Chang, S. Nitride-Based LEDs With High-Reflectance and Wide-Angle Ag Mirror + SiO2 /TiO2 DBR Backside Reflector. Journal of Lightwave Technology, 2011; 29(7), 1033-1038.

[6] Hsu, Y. P., Chang, S. J., Su, Y. K., Chang, C. S., Shei, S. C., Lin, Y. C., Kuo, C. H., Wu, L. W., and Chen, S. C. InGaN/GaN light-emitting diodes with a reflector at the backside of sapphire substrates. Journal of Electronic Materials, 2003; 32(5), 403-406.

[7] Yan, B., Tran, N. T., Jiun-Pyng, Y., and Shi, F. G. Can Junction Temperature Alone Characterize Thermal Performance of White LED Emitters? IEEE Photonics Technology Letters, 2011; 23(9), 555-557.

[8] You, J. P., He, Y., and Shi, F. G. Thermal management of high power LEDs: Impact of die attach materials. Proc., International Microsystems, Packaging, Assembly and Circuits Technology, 2007; 239-242.

[9] Shih, Y.-C., Kim, G., Huang, L., You, J.-P., and Shi, F. G. Role of Transparent Die Attach Adhesives for Enhancing Lumen Output of Midpower LED Emitters With Standard MESA Structure. IEEE Transactions on Components, Packaging and Manufacturing Technology, 2015; 5(6), 731-736.

[10] Muth, J. F., Lee, J. H., Shmagin, I. K., Kolbas, R. M., Casey, H. C., Keller, B. P., Mishra, U. K., and DenBaars, S. P. Absorption coefficient, energy gap, exciton binding energy, and

recombination lifetime of GaN obtained from transmission measurements. Applied Physics Letters, 1997; 71(18), 2572-2574.

[11] Kvietkova, J., Siozade, L., Disseix, P., Vasson, A., Leymarie, J., Damilano, B., Grandjean, N., and Massies, J. Optical Investigations and Absorption Coefficient Determination of InGaN/GaN Quantum Wells. Physica Status Solidi (A), 2002; 190(1), 135-140.

[12] Palmer, J. M. The measurement of transmission, absorption, emission, and reflection. Handbook of Optics, 1995; 2, 25.11.

[13] Xu, Z., Kumar, S., Jung, J. P., and Kim, K. K. Reflection Characteristics of Displacement Deposited Sn for LED Lead Frame. Materials Transactions, 2012; 53(5), 946-950.

[14] Dow Corning Corp. Dow Corning® OE-6630 Optical Encapsulant. 2015. http://www.dowcorning.com/applications/search/default.aspx?R=6577EN.

[15] Sun, C.-C., Chang, Y.-Y., Yang, T.-H., Chung, T.-Y., Chen, C.-C., Lee, T.-X., Li, D.-R., Lu, C.-Y., Ting, Z.-Y., Glorieux, B., Chen, Y.-C., Lai, K.-Y., and Liu, C.-Y. Packaging efficiency in phosphor-converted white LEDs and its impact to the limit of luminous efficacy. Journal of Solid State Lighting, 2014; 1(1), 1-17.

[16] Lin, Y.-H., You, J. P., Lin, Y.-C., Tran, N. T., and Shi, F. G. Development of High-Performance Optical Silicone for the Packaging of High-Power LEDs. IEEE Transactions on Components and Packaging Technologies. 2010; 33(4), 761-766.

[17] Fei, W., Peng, S., Jinlong, Z., Jianhua, Z., and Luqiao, Y. Effect of die-attach materials and thickness on the reliability of HP-LED. Proc., International Conference on Electronic Packaging Technology (ICEPT), 14th, 2013; 1048-1052.

[18] Tsai, M. Y., Chen, C. H., and Kang, C. S. Thermal analyses and measurements of low-Cost COP package for high-power LED. Proc., Electronic Components and Technology Conference, 58th, 2008; 1812-1818.

[19] Chang, M.-H., Das, D., and Pecht, M. Junction Temperature Characterization of High Power Light Emitting Diodes. Proc., IMAPS Mid-Atlantic Microelectronics Conference, 2011; 23-24.

[20] Li, W. A Study of Plasma-Cleaned Ag-Plated Cu Leadframe Surfaces. Journal of Electronic Materials. 2010; 39(3), 295-302.

[21] Choi, S., and Ma, B. Corrosive tendency of Ag plated lead frame applied to white LED. Proc., IEEE International Symposium on the Physical and Failure Analysis of Integrated Circuits (IPFA), 18th, 2011; 1-3.

CHAPTER 3

OPTICAL ROLE OF DIE BONDING

FOR CHIP-ON-BOARD WHITE LIGHT EMITTING DIODE EMITTERS

3.1. INTRODUCTION

Various methods to enhance optical efficiency of light emitting diodes (LEDs) have been introduced. Those include, at the LED chip fabrication level, multiple quantum well (MQW) thickness control [1], polarization matching at the active layers [2], advanced optical reflectors [3-5] and surface texturing [6-9]. On the other hand, the materials and processes for the packaging of LED emitters have also been continuously improved by improvement of leadframe reflectance [10], thermal management [11, 12], and optical properties for the encapsulant materials [13-15]. These improvements have driven solid state lightings industries to develop optically efficient designs in LED packaging methods. The Chip-on-board (COB) packaging for the LED emitters with various choices of sizes and output powers are now widely used for solid state lightings [16, 17] due to the advantages in thermal performance, compactness, and easiness of manufacturing for the light sources [17-19]. For the die bonding process, which is a part of LED packaging, a silver-mixed adhesive has been chosen mainly because of thermal and electrical conduction requirements. However, the mainstream LED chip used for lighting and backlighting is a low to mid-power (input current less than 150 mA) chip, thus the thermal dissipation of LED emitters with these mid-power

chips is not often limited by the thermal conduction between the chip and substrate, i.e., the die attach adhesive pathway [20]. Moreover, the mainstream LED chip is mesa type, thus no electrical conduction is required from the bottom of LED chip to the substrate. Therefore, dielectric adhesives (either optically transparent or translucent ones) can be used for the LED chip bonding. It has been demonstrated for white LED emitters packaged in a leadframe, the use of optically clear adhesive (CDAA) for replacing conventional silver-mixed DAA (Ag-DAA) can lead to a significant enhancement in the light output [21, 22]. The absorption of the sidewall emission due to higher DAA fillet coverage can be avoided by using CDAA, and the reliability test result by CDAA is equivalent to the Ag-DAA despite the difference of thermal resistance in between those two DAAs [21].

Hence, the objective of the present work is to investigate the role of DAA materials in influencing the light output for the COB white LED (WLED) emitters. It is found that the optical reflectance of the COB packaging board is strongly dependent on the DAA applied and the light output influence by materials and process parameters of the DAA is much stronger for multiple COB emitters. It is demonstrated for the first time that the light output of multiple chip-packaged COB white LED emitter using a CDAA exhibits a significant enhancement in light output up to 22 % compared to one using a conventional Ag-DAA.

3.2. APPROACH

A schematic cross-sectional drawing of a packaged COB WLED emitter by using a chip with standard mesa structure (Figure 3.1a) and the corresponding optical model for

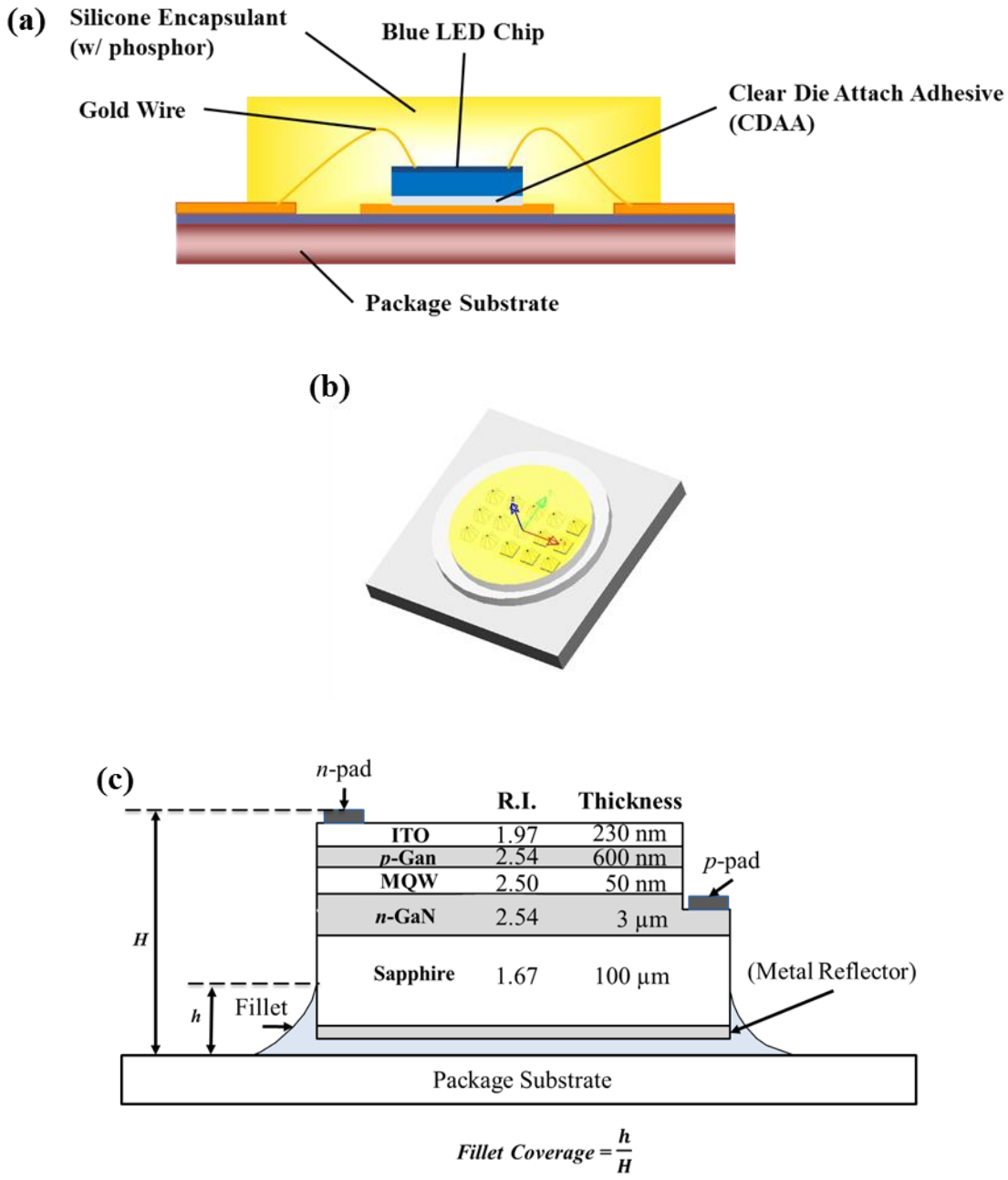

Figure 3.1. (a) Schematic cross section of a packaged COB WLED emitter by using optically clear die attach adhesive (CDAA). (b) Optical model used in Monte-Carlo simulations. (c) Schematic cross section of the chip and DAA layer. Relative refractive index for each chip layer is at 450 nm of wavelength. Fillet coverage of the DAA is defined by the height of covered DAA over the chip height.

the Monte Carlo simulation using *LightTools* (Figure 3.1b) are shown in Figure 3.1. Two million rays are employed in order to maintain simulation error less than 1 % for each simulation run. An input current of 120 mA is applied for each LED chip (24 × 24 mil in size) which has a dominant wavelength of 450 nm. The thickness of each layer and its respective relative refractive index [7] can be found in Figure 3.1c. The light output of the COB LED emitters influenced by the chip backside reflector (BR) is also considered. For the BR-based chip, commercially available LED chips with two different BR materials are selected: BR with the reflectivity of 98 % at 450 nm and Au based BR. Up to 15 LED chips are packaged for the multiple COB LED emitters. The light output is normalized by the number of chips packaged in order to investigate the influence of reduced light output by multiple chips and packaging conditions.

For the COB packaging boards, a flat package substrate [16, 17] is employed to compare the light output of the leadframe based emitter as a function of the reflectance of the package substrate [22]. The COB packaging board has the dimension of 9.5 × 9.5 × 0.9 mm, and the inner diameter of encapsulant region is 6 mm. The width and the height of outer dam for encapsulant packaging are 0.7 mm and 0.5 mm, respectively. [16] The reflectance for the package substrate (R_S) during the simulation ranges from 70 % to 99 % [23]. For the experimental samples, six groups of package substrates with different reflectance are employed. For each group of package substrate, the measured reflectance at the wavelength of 450 nm by USHIO URE-45V spectroscopic reflectometer is presented in Table 1. The silicone encapsulant has a relative refractive index of 1.53, and the optical transmittance is 99 % for 1 mm in thickness, at the wavelength of 450 nm [24]. For the WLED emitters, 11 wt. % of yellow phosphor powder with dominant peak wavelength of 535 nm is distributed

Table 3.1. Measured reflectance for the COB boards at the wavelength of 450 nm. The reflectance is measured by USHIO URE-45V spectroscopic reflectometer.

Index Group	A	B	C	D	E	F
Reflectance (%)	75.2	78.1	84.4	88.2	93.1	95.2

by mixing with the encapsulant, and resulted correlated color temperature (CCT) is 5,000 K [25]. For the Ag-DAA, commercially available Ag-mixed epoxy resin is used. The model of Ag-DAA used in simulations has the absorptance of 70% for the 1 mm thickness at the wavelength of 450 nm, which is obtained by mixing Ag particles with epoxy-based DAA matrix [21]. The CDAA used has an optical transmittance of 85 % for 1 mm in thickness: the relative refractive index is set at 1.53 for the wavelength of 450 nm [14, 22]. As the specifications for commercially available DAA materials, the bondline thickness of the CDAA and the Ag-DAA are taken to be 5 μm and 25 μm, respectively [26], and the fillet coverage by the DAA is set up to 40 % of the LED chip height. The DAA fillet coverage is defined by the chip height as much as the lower electrode of the chip with mesa structure, as illustrated in Figure 3.1c. The possible thermal-radiation coupling is not considered in the simulations because relatively lower power is involved in the present case of mid-power LEDs [27].

The packaging process for experimental measurement is as follows: (1) the package substrate is cleaned by isopropyl alcohol and baked at 75 °C before use; (2) a blue LED chip is attached to the package substrate by using DAAs. Musashi ML-808 dispenser and

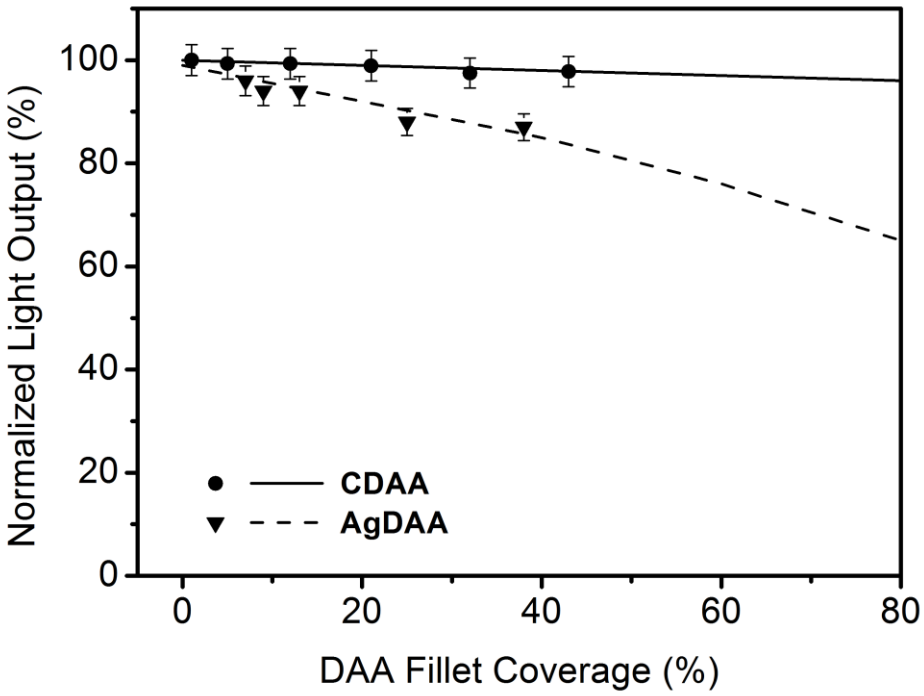

Figure 3.2. Light output of blue LED emitters encapsulated with silicone encapsulant as a function of DAA fillet coverage. The Optically clear DAA is denoted as CDAA and the conventional DAA with silver paste is denoted as Ag-DAA.

Shotmaster desptop dispensing robot are used for precise dispension; (3) the samples are cured at 150 °C for 2 hours; (4) wire-bonding is performed for interconnect between the LED chip and the pads on the package substrate; (5) silicone encapsulant is injected into the chip-packaged area; (6) the samples are cured at 150 °C for 2 hours; (7) the packaged LED emitters are then mounted on a heat sink and wired. Keithley 2400 power generator with constant current mode of 120 mA is used. Light output of packaged LED emitters is measured

in LabSphere integrating sphere by Instrument Systems CAS 140CT compact array spectrometer.

The simulated results for the light output as a function of BR reflectance (R_{BR}) for the packaged blue COB LED emitters are compared with the experimental data to verify optical model. As shown in Figure 3.2, light output of the packaged emitter is not hindered by CDAA whereas a substantial amount of photoemission is absorbed and hence reduced by Ag-DAA with increased fillet coverage. This tendency is same as the results from leadframe-based SMD type LED emitters [22].

3.3. RESULT AND DISCUSSION

3.3.1. Light Output by the Reflectance of Package Substrate: Single-chip COB LED Emitters using CDAA

The light output of single-chip COB and leadframe-type LED emitters by the CDAA for the chip bonding as a function of the reflectance of package substrate (R_S) are shown in Figure 3.3. The results are normalized by the light output of the LED emitter with the BR-based (R_{BR} = 98 %) chip at R_S of 98 % [22]. The correlated color temperature is 5,000 K for the WLED emitters. The results show that the light output for the COB emitter exhibits the same tendency as the leadframe type emitter as a function of R_S. The emitter with the BR-based chip (R_{BR} = 98%) exhibits the highest light output. However, it is observed that the emitter with the BR-free chip shows higher light output than the emitter with Au-BR. It is shown that the lumen output of using BR-free chip and CDAA is strongly influenced by the R_S, hence it is still a dominant parameter even for a COB LED emitter to achieve higher light

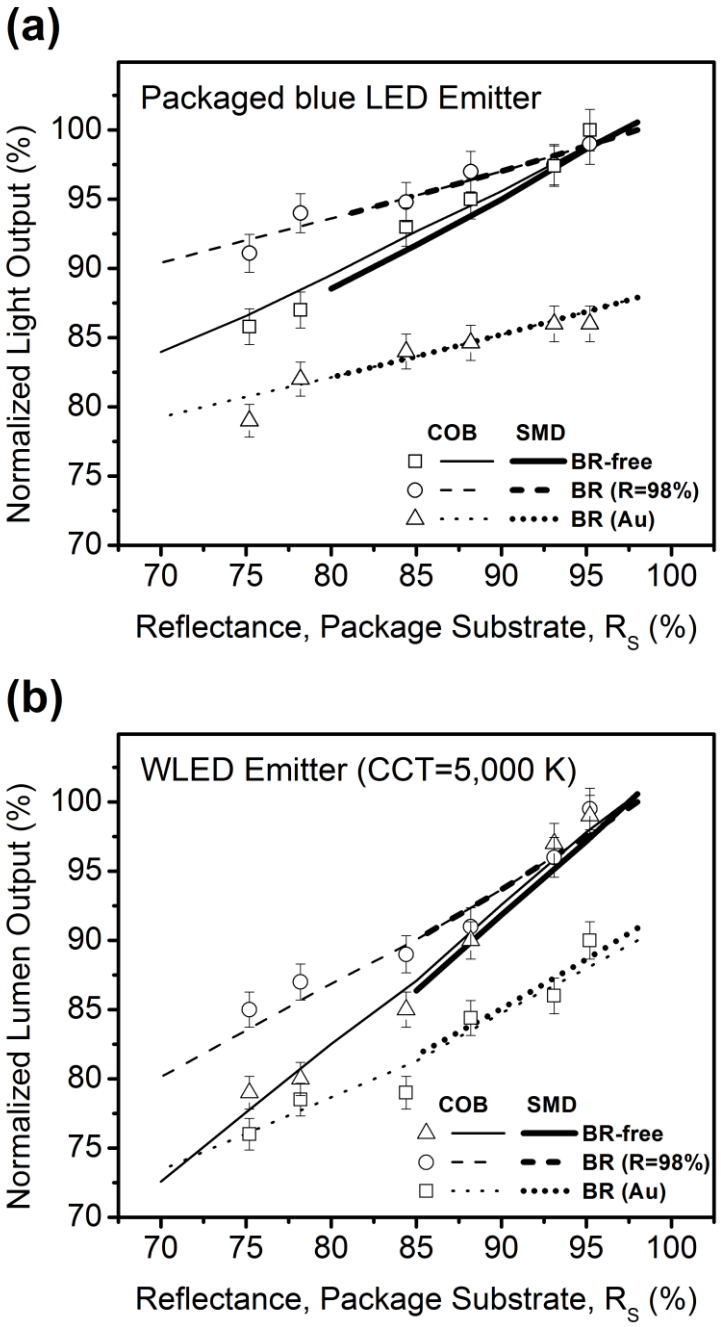

Figure 3.3. Light output of (a) a blue LED and (b) a white LED COB and leadframe-based emitters as a function of reflectance of the package substrate (R_S). CCT is set to 5,000 K. CDAA is used and the fillet coverage is 40 %. Simulation results for COB-LED emitters are compared to leadframe based SMD LED emitters [22]. Results are normalized by the light output of BR (R_{BR} =98 %) based emitter at R_S of 98 %.

output. This requires the package substrate to achieve higher reflectance in order to enhance the overall lumen output by taking the advantage of using BR-free chips.

3.3.2. Light Output influenced by DAAs: The Number of Packaged LED Chips for multiple COB WLED Emitters

The light output of COB WLED emitters by using CDAA and Ag-DAA as a function of the number of packaged chips on board is plotted in Figure 3.4. For the COB packaging board, sample group C is used for the emitter samples, and the R_S is set to 84.4 % for simulations, to match the reflectance with the measurement. The results are normalized by the light output of the emitter with the BR-based chip at R_{BR} of 98 %. For multiple COB LED emitters, each light output is also normalized by the light output of the single chip emitter.

$$P_{Normalized} = \frac{P_{Multi}}{N * P_{Single}} \quad (1)$$

The results show that increasing the number of chips reduces light output. For the CDAAs with the fillet coverage of 0 %, the amount of reduced light output due to increased number of chips by using BR-based and BR-free chips are 9.1 % and 5.5 %, respectively. This tendency is maintained while the fillet coverage of CDAA is increased, as shown in Figure 3.4(b). For the CDAAs with the fillet coverage of 40 %, light output for BR-based and BR-free emitters is reduced as much as 13.2 % and 10 %, respectively, for the multiple chips. The BR-based emitter with R_{BR} of 98 % shows higher light output than the BR-free emitter with the CDAA. However, the role of the BR for the packaged COB emitter is further diminished by

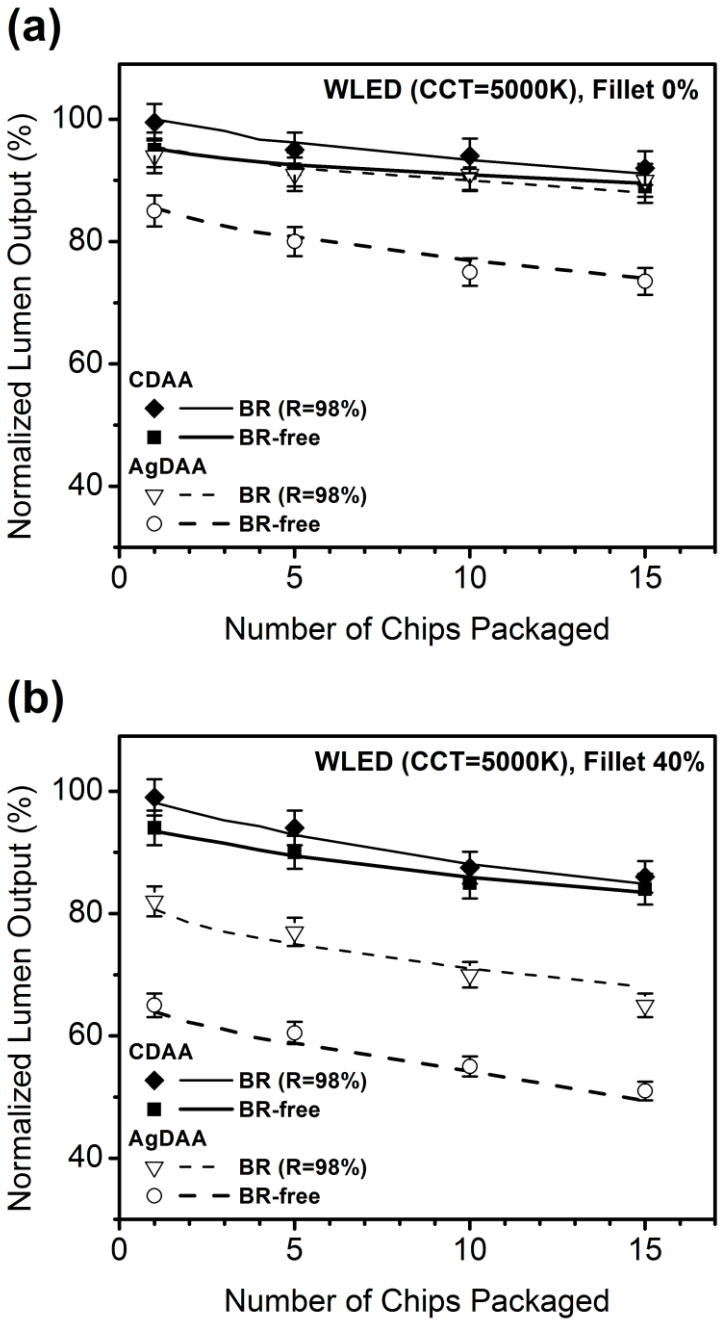

Figure 3.4. Light output of COB WLED emitters (CCT = 5, 000 K) packaged with (a) Fillet coverage of 0 % and (b) 40 % for DAA materials as a function of the number of packaged chips. The light output is normalized by the number of chips packaged. The reflectance of the package substrate (R_S) is 84.4 %. Results are normalized by the light output of single-chip emitter with 0 % fillet-CDAA.

increasing number of chips because the light absorption by the CDAA is much lower than Ag-DAA. On the other hand, in case of the fillet coverage is 0 %, the light output for BR-based and BR-free emitters with multiple chip is rather enhanced regardless the DAA materials. Thus, it is evident that the fillet coverage is a crucial packaging parameter for the enhancement in lumen output. As a result, the enhancement in light output due to the replacement of the DAA material from a conventional Ag-DAA to a CDAA is 22 % in case of the 15-chip-on-board white LED emitter. Ag-based conventional DAA is also an absorption source, and the light output of the BR-free emitter is severely reduced due to the downward absorption. This light absorption by the Ag-DAA is even worse in case of the fillet coverage of 40 % as shown in Figure 3.4(b).

3.3.3. Light Output for Multiple COB LED Emitters by LED Chip Spacing

Figure 3.5 presents the simulation result of 15-chip packaged multi-COB emitter. light output of COB WLED emitters by using BR-free chip and BR based chip with R_{BR} of 98 % as a function of the distance between the chips packaged. CDAA is used for simulations. The R_S is set to 84.4 %, and the results are normalized by the light output of the BR based emitter at R_S of 98 %. Chip spacing is set up to 1.4 mm due to the size restriction of the package substrate used in simulations. For the CDAA based emitter with 0 % of fillet coverage, the results show that the light output is enhanced up to 23% by the chip spacing from 0.65 mm to 1.4 mm. For 40 % of the fillet coverage, the light output exhibits maxima at about 1.0 mm. This maximum is based on increased amount of CDAA material for packaging, which is an absorption source. The BR based emitter exhibits up to 2.96 % higher light output than the BR-free based emitter, however it is a much lower enhancement with respect to either a

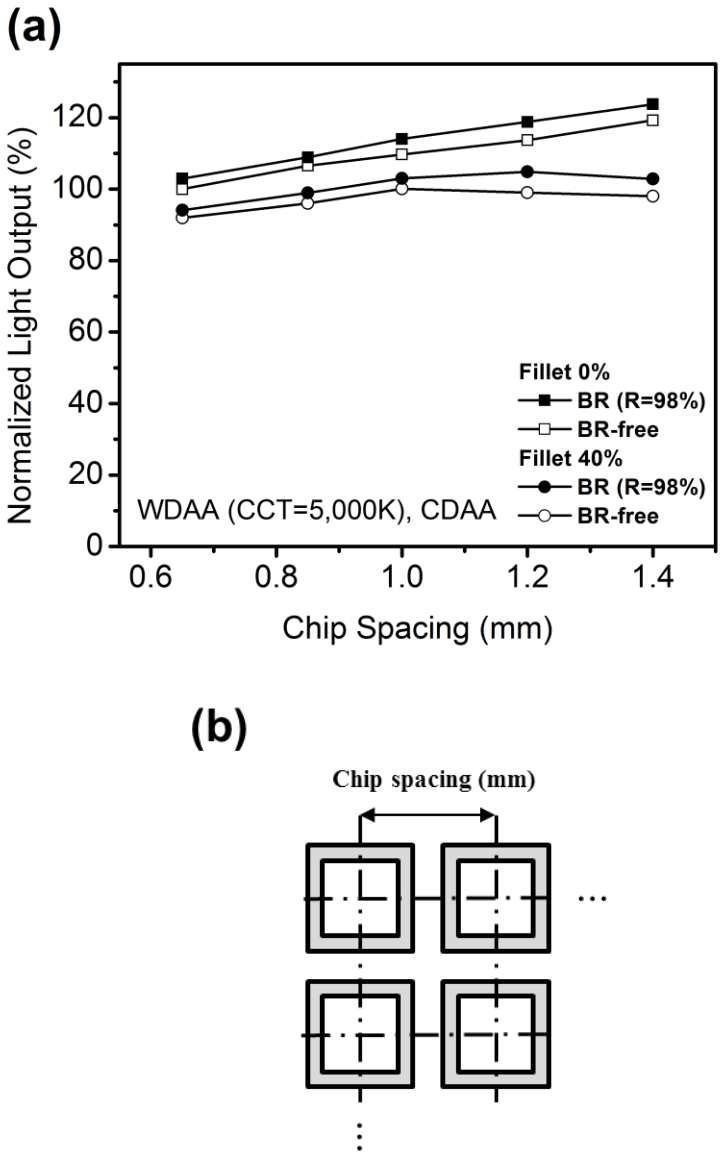

Figure 3.5. (a) Light output of COB WLED emitters (CCT = 5, 000 K, 15 chips) packaged with CDAA using BR-free and BR based chip (R_{BR}=98%) as a function of chip spacing. The reflectance of the package substrate (R_S) is 84.4 %. Results are normalized by the light output with zero-fillet CDAA. (b) Definition of chip spacing. The inter distance in between chips are identical.

naked chip or leadframe based emitter.

3.4. CONCLUSIONS

The optical role of packaging material and process parameters for the packaged COB LED emitter in order to enhance light output were investigated. It is demonstrated for multiple COB LED emitters that the use of optically clear adhesive for replacing conventional silver-mixed DAA can lead to a significant enhancement in the light output. The role of chip backside reflector for the multiple COB LED emitter is even more diminished. The light output of a multiple COB LED emitter is strongly influenced by packaging materials and processing, and therefore the light output can be enhanced by optimization of these packaging parameters.

REFERENCES

[1] Y.-L. Li, Y.-R. Huang, and Y.-H. Lai, "Efficiency droop behaviors of InGaN/GaN multiple-quantum-well light-emitting diodes with varying quantum well thickness," Applied Physics Letters, vol. 91, p. 181113, 2007.

[2] M. F. Schubert, J. Xu, J. K. Kim, E. F. Schubert, M. H. Kim, S. Yoon, S. M. Lee, C. Sone, T. Sakong, and Y. Park, "Polarization-matched GaInN/AlGaInN multi-quantum-well light-emitting diodes with reduced efficiency droop," Applied Physics Letters, vol. 93, p. 041102, 2008.

[3] Y. P. Hsu, S. J. Chang, Y. K. Su, C. S. Chang, S. C. Shei, Y. C. Lin, C. H. Kuo, L. W. Wu, and S. C. Chen, "InGaN/GaN light-emitting diodes with a reflector at the backside of sapphire

substrates," Journal of Electronic Materials, vol. 32, pp. 403-406, 2003/05/01 2003.

[4] J. K. Kim, J. Q. Xi, and E. F. Schubert, "Omni-directional reflectors for light-emitting diodes," 2006, pp. 61340D-61340D-12.

[5] N. M. Lin, S. Shei, and S. Chang, "Nitride-Based LEDs With High-Reflectance and Wide-Angle Ag Mirror + SiO_2 /TiO_2 DBR Backside Reflector," Lightwave Technology, Journal of, vol. 29, pp. 1033-1038, 2011.

[6] H. W. Huang, C. H. Lin, C. C. Yu, B. D. Lee, C. H. Chiu, C. F. Lai, H. C. Kuo, K. M. Leung, T. C. Lu, and S. C. Wang, "Enhanced light output from a nitride-based power chip of green light-emitting diodes with nano-rough surface using nanoimprint lithography," Nanotechnology, vol. 19, p. 185301, 2008.

[7] Y.-S. Lin and J. A. Yeh, "GaN-Based Light-Emitting Diodes Grown on Nanoscale Patterned Sapphire Substrates with Void-Embedded Cortex-Like Nanostructures," Applied Physics Express, vol. 4, p. 092103, 2011.

[8] H. Chen, H. Guo, P. Zhang, X. Zhang, H. Liu, S. Wang, and Y. Cui, "Enhanced Performance of GaN-Based Light-Emitting Diodes by Using Al Mirror and Atomic Layer Deposition-TiO_2 /Al_2O_3 Distributed Bragg Reflector Backside Reflector with Patterned Sapphire Substrate," Applied Physics Express, vol. 6, p. 022101, 2013.

[9] H. Guo, H. Chen, X. Zhang, P. Zhang, J. Liu, H. Liu, and Y. Cui, "High-performance GaN-based light-emitting diodes on patterned sapphire substrate with a novel hybrid Ag mirror and atomic layer deposition-TiO_2/Al_2O_3 distributed Bragg reflector backside reflector," Optical Engineering, vol. 52, pp. 063402-063402, 2013.

[10] Y. Shao, Y.-C. Shih, G. Kim, and F. G. Shi, "Study of optimal filler size for high performance polymer-filler composite optical reflectors," Optical Materials Express,

vol. 5, pp. 423-429, 2015/02/01 2015.

[11] B. Yan, J. P. You, N. T. Tran, Y. He, and F. G. Shi, "Influence of Die Attach Layer on Thermal Performance of High Power Light Emitting Diodes," Components and Packaging Technologies, IEEE Transactions on, vol. 33, pp. 722-727, 2010.

[12] B. Yan, N. T. Tran, Y. Jiun-Pyng, and F. G. Shi, "Can Junction Temperature Alone Characterize Thermal Performance of White LED Emitters?," Photonics Technology Letters, IEEE, vol. 23, pp. 555-557, 2011.

[13] Y.-C. Lin, Y. Zhou, N. Tran, and F. Shi, "LED and Optical Device Packaging and Materials," in Materials for Advanced Packaging, D. Lu and C. P. Wong, Eds., ed: Springer US, 2009, pp. 629-680.

[14] Y.-H. Lin, J. P. You, Y.-C. Lin, N. T. Tran, and F. G. Shi, "Development of High-Performance Optical Silicone for the Packaging of High-Power LEDs," Components and Packaging Technologies, IEEE Transactions on, vol. 33, pp. 761-766, 2010.

[15] E. Juntunen, O. Tapaninen, A. Sitomaniemi, and V. Heikkinen, "Effect of Phosphor Encapsulant on the Thermal Resistance of a High-Power COB LED Module," Components, Packaging and Manufacturing Technology, IEEE Transactions on, vol. 3, pp. 1148-1154, 2013.

[16] Citizen, "Data Sheet CLL010-0305A1-50KL1A1," vol. Avaliable: http://ce.citizen.co.jp/lighting_led/en/products/.

[17] Lightspot Technology Group Co., Ltd, "Integrated multi-chip packaging technology," Avaliable: www.COB-LED.com.

[18] M. Y. Tsai, C. H. Chen, and C. S. Kang, "Thermal analyses and measurements of low-Cost COP package for high-power LED," in Electronic Components and Technology

Conference, 2008. ECTC 2008. 58th, 2008, pp. 1812-1818.

[19] Y. Hui, S. Jintang, X. Chao, L. Xinhu, L. Jingdong, Z. Li, and L. Chiming, "Chip-on-board (COB) wafer level packaging of LEDs using silicon substrates and chemical foaming process(CFP)-made glass-bubble caps," in Electronic Packaging Technology and High Density Packaging (ICEPT-HDP), 2011 12th International Conference on, 2011, pp. 1-4.

[20] Y. Bohan, Y. Jiun-Pyng, N. T. Tran, H. Yongzhi, and F. G. Shi, "Influence of Die Attach Layer on Thermal Performance of High Power Light Emitting Diodes," Components and Packaging Technologies, IEEE Transactions on, vol. 33, pp. 722-727, 2010.

[21] Y.-C. Shih, G. Kim, L. Huang, J.-P. You, and F. G. Shi, "Role of Transparent Die Attach Adhesives for Enhancing Lumen Output of Midpower LED Emitters With Standard MESA Structure," Components, Packaging and Manufacturing Technology, IEEE Transactions on, vol. 5, pp. 731-736, 2015.

[22] G. Kim, Y.-C. Shih, J.-P. You, and F. G. Shi, "Optical role of die attach adhesive for white LED emitters: light output enhancement without chip-level reflectors," Journal of Solid State Lighting, vol. 2, pp. 1-8, 2015.

[23] Z. Xu, S. Kumar, J. P. Jung, and K. K. Kim, "Reflection Characteristics of Displacement Deposited Sn for LED Lead Frame," MATERIALS TRANSACTIONS, vol. 53, pp. 946-950, 2012.

[24] DowCorningCorp, "Dow Corning® OE-6630 Optical Encapsulant," Available: http://www.dowcorning.com/applications/search/default.aspx?R=6577EN.

[25] C.-C. Sun, Y.-Y. Chang, T.-H. Yang, T.-Y. Chung, C.-C. Chen, T.-X. Lee, D.-R. Li, C.-Y. Lu, Z.-Y. Ting, B. Glorieux, Y.-C. Chen, K.-Y. Lai, and C.-Y. Liu, "Packaging efficiency in

phosphor-converted white LEDs and its impact to the limit of luminous efficacy," Journal of Solid State Lighting, vol. 1, pp. 1-17, 2014/11/18 2014.

[26] W. Fei, S. Peng, Z. Jinlong, Z. Jianhua, and Y. Luqiao, "Effect of die-attach materials and thickness on the reliability of HP-LED," in Electronic Packaging Technology (ICEPT), 2013 14th International Conference on, 2013, pp. 1048-1052.

[27] M.-H. Chang, D. Das, and M. Pecht, "Junction Temperature Characterization of High Power Light Emitting Diodes," in IMAPS Mid-Atlantic Microelectronics Conference, 2011.

CHAPTER 4

ROLE OF PACKAGING AND MATERIALS

IN TRANSPARENT SUBSTRATE-BASED OMNIDIRECTIONAL COB-WLED EMITTERS

4.1. INTRODUCTION

The light emitting diode (LED) emitters using chip-on-board (COB) packaging technology have been widely used for solid state lightings due to the advantages in thermal management, compactness, and easiness of manufacturing [1-3]. In a conventional COB-LED emitter, the LED die is directly bonded onto a reflective substrate. The die with a chip-level backside reflector (BR) is often used in order to enhance the optical performance. The design for the conventional LED emitter aims the photons to be guided upwards, hence the optical performance of each emitter is strongly influenced by the reflectivity of the packaging components, especially by the reflective substrate. Unlike the conventional COB-LED emitters, the transparent substrate-based filament type white LED (WLED) emitter is made of a linear array of low-power (less than 0.05 W) LED dies onto an optically transparent substrate as shown in Figure 4.1 [4]. The BR-free die is bonded onto the substrate using an optically transparent die attach adhesive. Therefore, this filament type linear transparent substrate-based COB-WLED emitter enables omnidirectional light emission. Owing to this unique optical characteristic, these linear COB-WLED emitters are able to replace traditional tungsten filaments in the incandescent bulbs. A simplified structure of his linear COB-WLED

emitter is another advantage. Unlike previously introduced WLED-based light bulbs, the filament type linear COB-WLED emitters do not require bulky fixtures such as second optics or heatsinks [5, 6], hence this simple structure can achieve lower manufacturing cost with only a few modifications on the filament based traditional incandescent bulb manufacturing as well as to meet the cosmetic needs required to the decorative lightings.

Despite those merits, this transparent substrate-based COB-WLED emitter is still facing challenges. Even though the light bulb using linear WLED emitters has a simplified structure, the price is still too high to be widely accepted by end users. The lumen output as well as thermal management of the light bulb using linear COB-WLED emitters still needs to be improved. Hence, this work presents, for the first time, an investigation of possible packaging and materials optimization of transparent substrate-based COB-WLED emitters with an objective to enhance the lumen performance. In terms of the role of packaging and materials in transparent substrate based COB-WLED emitters, it is found that the lumen output is greatly enhanced up to 26 %. if the transparent substrate is optimized with respect to its dimensions. It is also found that the optically transparent die attach adhesive is preferred over optically reflective one. In addition, an optimization of the refractive index of die attach adhesive, as well as optimization of LED die spacing and phosphor layer structure contribute significantly in enhancing the lumen output.

4.2. APPROACH

Figure 4.1a presents a schematic drawing of the filament type lighting using linear COB-WLED emitters. A schematic cross-sectional drawing of the transparent substrate-

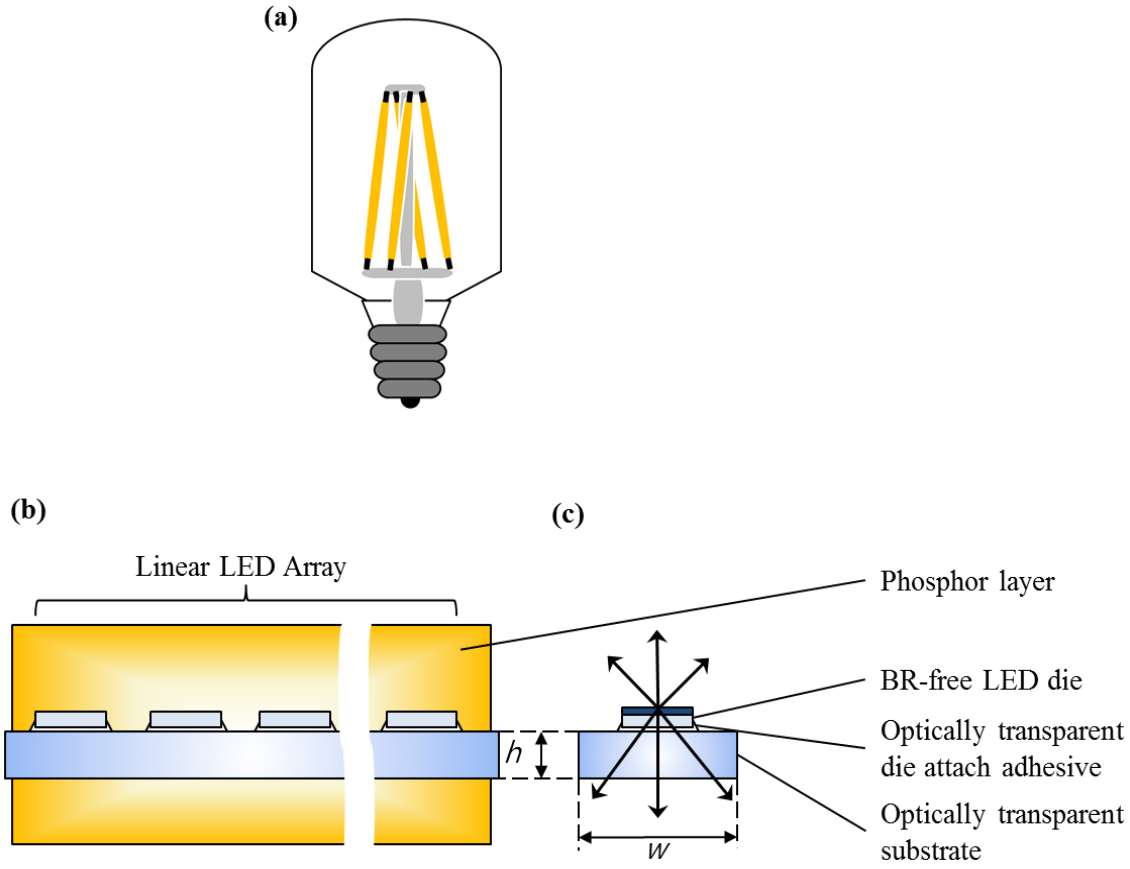

Figure 4.1. (a) schematic drawing of the filament type lighting using transparent substrate-based linear COB-WLED emitters. (b) schematic cross-sectional drawings of the transparent substrate-based linear COB-WLED emitter. (c) the light emission from a transparent substrate-based COB-LED emitter. A backside reflector (BR)-free LED die is bonded onto the substrate using optically transparent die attach adhesive for omnidirectional light emission.

based linear COB-WLED emitter used in this work is also illustrated in Figure 4.1b. The refractive index of the transparent substrate is ranging from 1.42 to 1.8 at 450 nm of the wavelength. The length of the transparent substrate is 38 mm, the width (denoted as w) and the thickness (denoted as h) are adjusted to optimize lumen output of the emitter. The blue LED die (0.25 mm × 0.4 mm in size and 0.03 W in power) in standard mesa structure, with a dominant wavelength of 450 nm and the thickness of each layer and its respective relative refractive index are referred by the previous work [7]. The absorption coefficient for the GaN and the multiple quantum well (MQW) is 200 cm-1 and 3600 cm-1, respectively [8, 9]. An array of 28 LED dies is bonded by using the optically transparent die attach adhesive (CDAA) [10] or a reflective polymer-filler composite white DAA (WDAA) using Al2O3 [11]. The transmittance of the CDAA is 85 % for the sample thickness of 1 mm at the wavelength of 450 nm [12]. The fillet coverage for the DAA is set of 50 %. The phosphors with dominant peak wavelength of 535 nm and 630 nm are dispersed within the encapsulant, and the target CCT is 2,700 K. To elucidate the detailed impact of packaging processes and materials, Monte-Carlo simulations using *LightTools 8.0.3* are employed, and 2,000,000 rays are traced to control simulation error to be less than 1 % for each simulation run. The possible thermal-radiation coupling is not considered in the simulations because relatively lower power is involved in the present case of low-power LEDs [13].

4.3. RESULT AND DISCUSSION

Figure 4.2 presents the optimization of the LED die spacing on the lumen output of the transparent substrate-based linear COB-WLED emitter. An LED array of 5 dies is

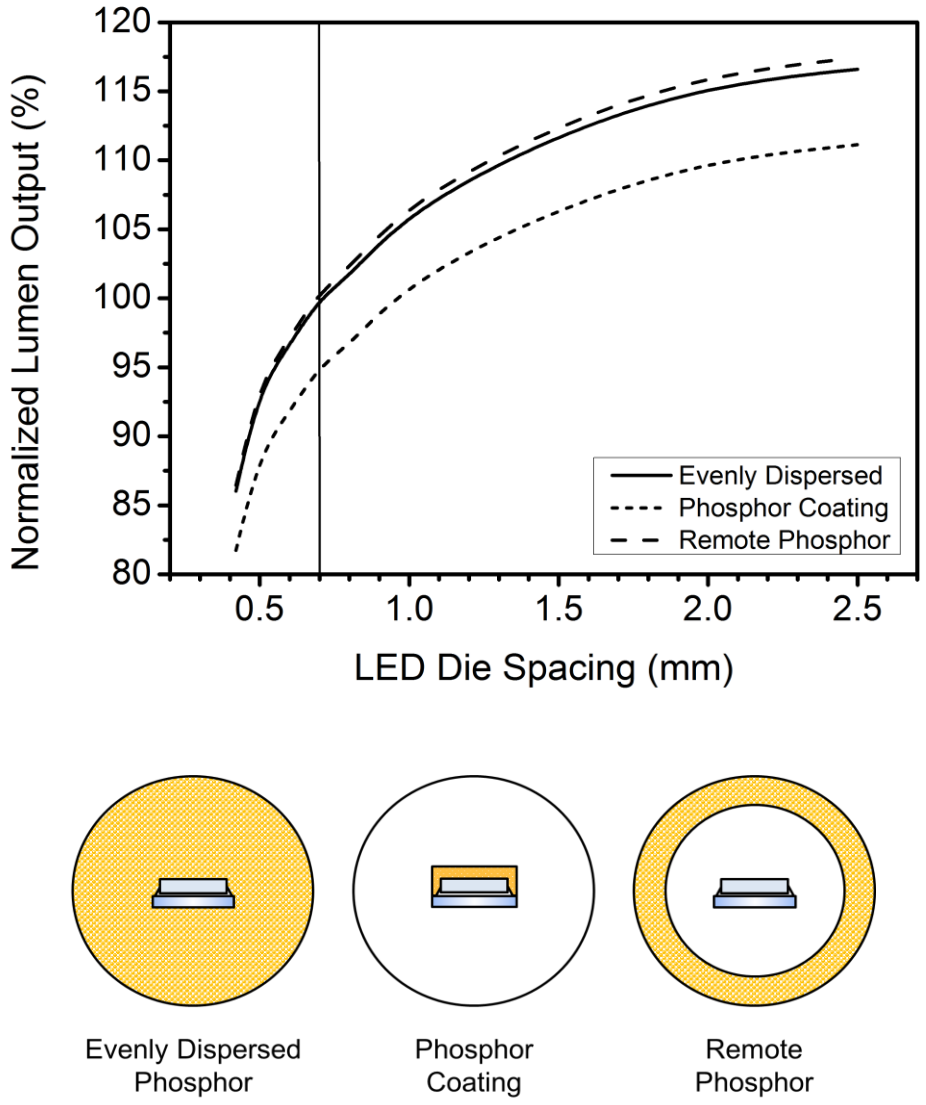

Figure 4.2. (a) Optimization of die spacing: the lumen output of the transparent substrate-based linear COB-WLED emitter as a function of the die spacing. An LED array of 5 dies is bonded onto the transparent substrate. Targeted CCT is set of 2,700 K. The lumen output is normalized as 100 % by the die spacing of 0.7 mm with evenly dispersed phosphor.

bonded onto the transparent substrate, and the targeted CCT is set of 2,700 K. the range of die spacing is set from 0.38 mm to 2.5 mm. The outer diameter is set of 3 mm, and three different phosphor settings are employed as shown: evenly dispersed phosphor, conformal phosphor coating and remote phosphor. The lumen output is normalized as 100 % by the die spacing of 0.7 mm with evenly dispersed phosphor [4]. The result shows that the lumen output is strongly influenced by the die spacing. The reduced lumen output by decreased die spacing from 0.7 mm to 0.42 mm is 14 %. This is because the light emission is absorbed by the GaN layers of adjacent dies. Thus it is evident that an optimization in die spacing is required to achieve maximized lumen output in case of the multiple COB-LED emitter. The optimization shows the enhancement of the lumen output by increased die spacing from 0.7 mm to 2.5 mm is 16.6%. and the tendency of enhancement is saturated as increased die spacing. Thus, the further die spacing than an existing specification is preferred, and this is a trade-off parameter with other manufacturing specifications. The results also present the lumen output of the linear COB-WLED emitters with evenly dispersed phosphor and remote phosphor are equivalent each other, while the conformal phosphor coating linear COB-WLED emitter exhibits 4.9 %. lower lumen output. This is because the conformal phosphor layer with high concentration scatters photons backwards to be absorbed by the GaN layer of the dies whereas the other cases secure enough spaces for more photons to be extracted. The tendency of different lumen output by phosphor settings is maintained through the following optimizations.

Figure 4.3 presents the optimization of the optical properties of transparent substrate. The effect of refractive index for the transparent substrate on lumen output of the transparent substrate-based linear COB-WLED emitter is shown with three different

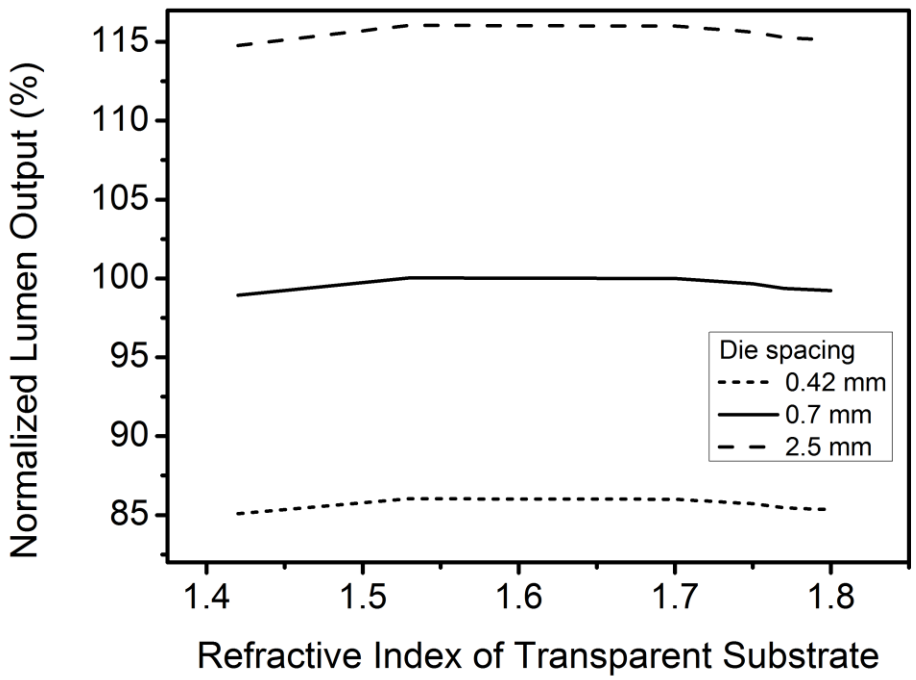

Figure 4.3. Optimization of the optical properties of transparent substrate: the lumen output of the linear COB-WLED emitter with evenly dispersed phosphor as a function of the refractive index of the transparent substrate. The width and thickness of the transparent substrate is 1.5 mm and 0.75 mm, respectively. The lumen output is normalized as 100 % by the one with the refractive index of 1.75.

die spacing: 0.42 mm, 0.7 mm and 2.5 mm. The width (w) and thickness (h) of the transparent substrate is 1.5 mm and 0.75 mm, respectively. The refractive index of the transparent substrate is ranging from 1.42 to 1.8. It is observed that the lumen output is maximized at 1.53 and 1.75, regardless the die spacing. These peaks show that the more photons are extracted when the refractive index of the transparent substrate is matched with either the encapsulant or the sapphire substrate of the LED die. Since the thermal conductivity of the sapphire is higher than glass, the sapphire substrate is considered as a suitable transparent substrate for the linear COB-WLED emitter [14]. The lumen output is normalized as 100 % by the maximum value for further optimization process.

Figure 4.4 presents the optimization of the geometry of the transparent substrate on lumen output of the transparent substrate-based linear COB-WLED emitter. The xy-plane represents the width (x-axis) and the thickness (y-axis) of the transparent substrate, respectively. The refractive index of the transparent substrate is 1.75, which is matched with the sapphire substrate of the LED die. The range of the width of the transparent substrate is set from 0.4 mm to 1.5 mm, and the range of the thickness is set from 0.1 mm to 0.75 mm. The lumen output is normalized as 100 % by the width and thickness of the transparent substrate at 1.5 mm and 0.75 mm, respectively. It is shown that the lumen output is increased by reduced width and thickness of the transparent substrate. The enhancement in lumen output by reduced optical dimensions is up to 26 %. It is significant that a simple modification in dimensions of the transparent substrate promote more light extraction to the encapsulation region. Therefore, thin and narrow transparent substrate for the linear COB-WLED emitter is preferred to achieve the higher lumen performance by enhanced light extraction efficiency of the transparent substrate.

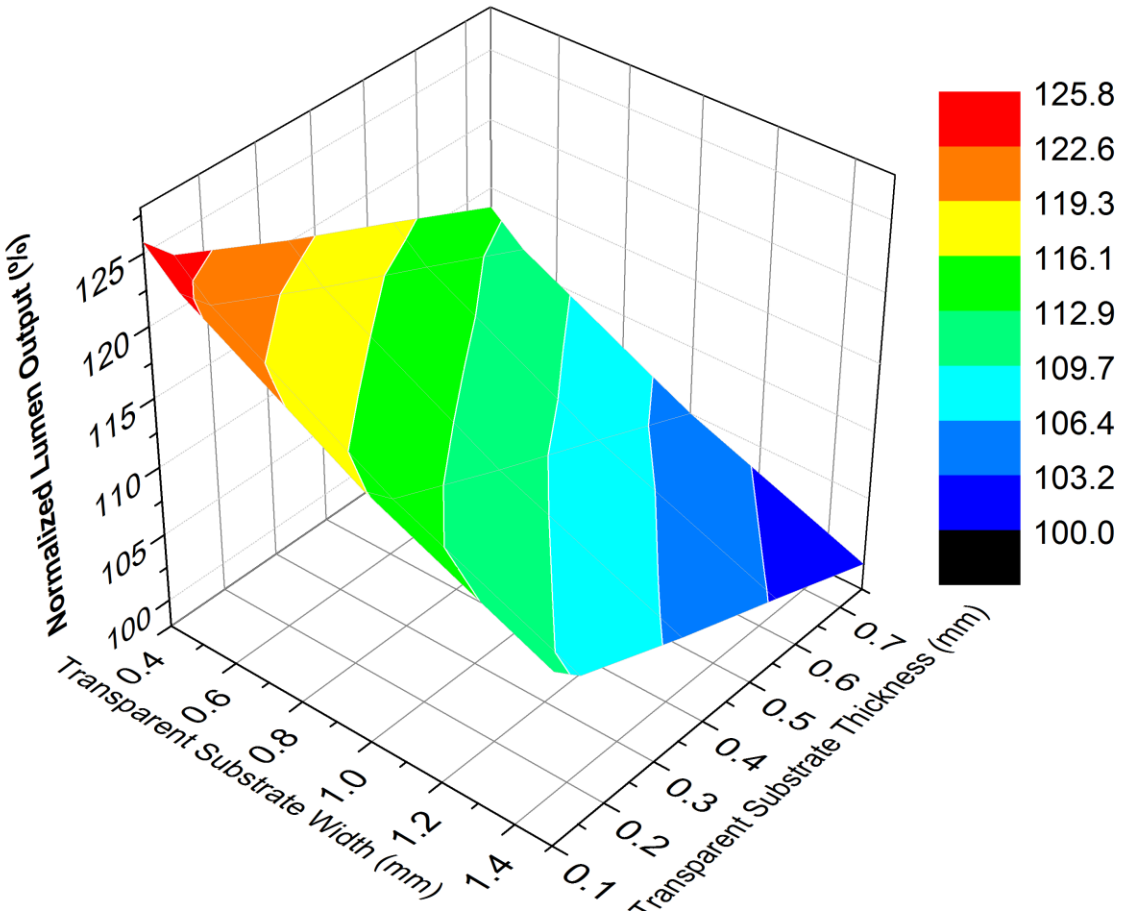

Figure 4.4. Optimization of the geometry of transparent substrate: the lumen output of the linear COB-WLED emitter in terms of the geometry of the transparent substrate. The normalized lumen output (z-axis) is shown as a function of the width (x-axis) and the thickness (y-axis) of the transparent substrate. The refractive index of the transparent substrate is 1.75. The lumen output is normalized as 100 % by the width and thickness of the transparent substrate at 1.5 mm and 0.75 mm, respectively.

Figure 4.5 presents the optimization of die attach adhesives (DAAs) on the lumen output of the transparent substrate-based linear COB-WLED emitter in terms of the ratio of the refractive index, the DAA over the substrate layers. Since the DAA is placed in between the LED die and the transparent substrate, the optical parameter of the DAA material is one of the factors which influences the lumen output of the linear COB-WLED emitter. CDAA and WDAA are applied on the optimized transparent substrate for die bonding. The bond line thickness of CDAA and WDAA are 4 μm and 9 μm, respectively. The lumen output is normalized at 100 % by the case using the CDAA with the ratio of refractive index (n_{DAA} / $n_{Substrate}$) of 1.0 and the fillet coverage of 0 %. The result shows that the lumen output of the linear COB-WLED emitter is maximized by the matched refractive index of the CDAA with the substrate, and it is little dependent on the fillet coverage due to the optical geometry which is involving the transparent substrate and the CDAA. On the other hand, the effect of refractive index for the WDAA matrix is insignificant, whereas the lumen output is strongly dependent on the fillet coverage. The WDAA promotes more photons to be reflected at the WDAA and sapphire interface, so that some of the reflected photons are re-absorbed by the GaN layers. Since the fillet formation is more critical to yield and reliability as well as uniform light distribution for the multi-die packaging in small size [15], CDAA is more desirable for the die bonding process of the linear COB-WLED emitter than WDAA.

Figure 4.6 presents the optimization of the thickness of the phosphor layer on the lumen output of the transparent substrate-based linear COB-WLED emitter. The thickness of the phosphor layer is described as the outer diameter of the phosphor layer. The targeted CCTs are set of 2,700 K, 5,000 K and 7,000 K. The lumen output is normalized as 100 % by the linear COB-WLED emitter with outer diameter of 1 mm. By ranging the outer

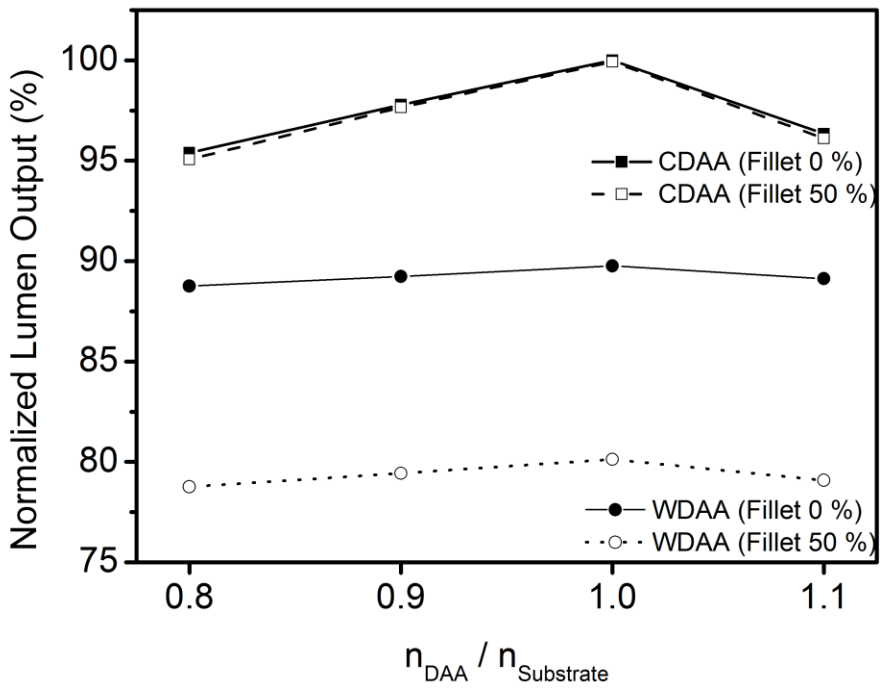

Figure 4.5. Optimization of packaging materials and process parameters: the lumen output of the transparent substrate-based linear COB-WLED emitters using optically clear die attach adhesive (CDAA) and optical reflective white DAA (WDAA) for die bonding, as a function of the ratio of refractive index, the DAA over the substrate. The bond line thickness for the CDAA and WDAA is 4 μm and 9 μm, respectively.

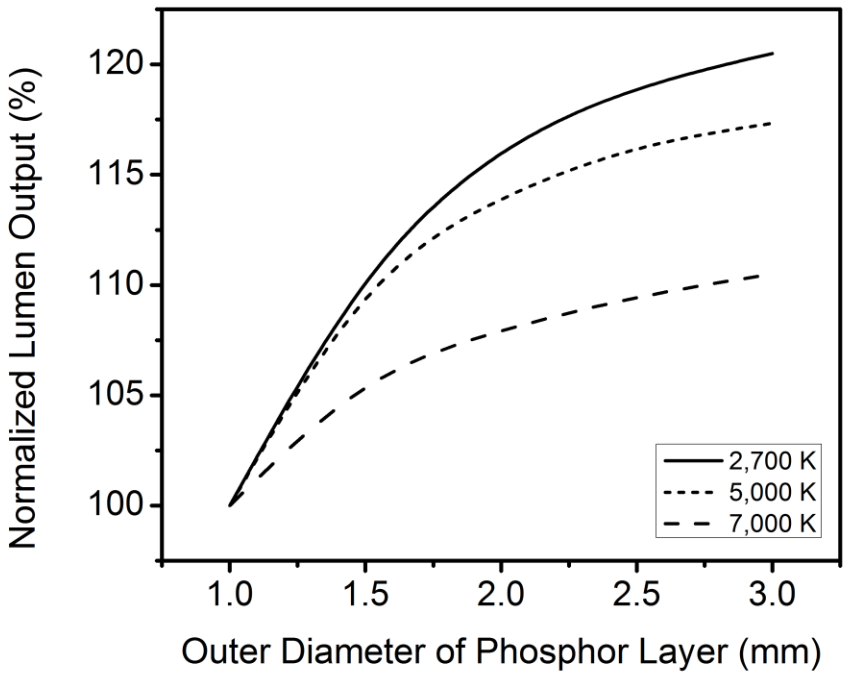

Figure 4. 6. Optimization of phosphor layer: the lumen output of the transparent substrate-based linear COB-WLED emitters as a function of the phosphor layer thickness. Targeted CCTs are 2,700 K, 5,000 K and 7,000 K. The lumen output is normalized as 100 % by the outer diameter of the phosphor layer of 1 mm.

diameter from 1 mm to 3 mm, the lumen output of 2,700 K is enhanced up to 20 %. due to less amount of back scattered photons by more dilute phosphor dispersed within the larger volume. This reduces photons to be trapped within or to be absorbed by the GaN layer of the dies. The tendency of the effect of the thickness of the phosphor layer on the lumen output is maintained for other targeted CCTs. Thus, the larger volume of the phosphor layer is preferred as much as the manufacturing specifications allow.

4.4. CONCLUSIONS

In this work, the effect of optimized materials and packaging parameters of the transparent substrate on the lumen output of the transparent substrate-based linear COB-WLED emitter has been investigated by Monte-Carlo ray tracing simulations. It is demonstrated that a simple modification in optical geometry of the transparent substrate is a critical parameter for the linear COB-WLED emitter to enhance lumen output. Optimized packaging materials and the process parameters are also investigated. Although this study focuses on simulations in order to systemize the parameters, the findings may well have a bearing on influences in lumen output for the transparent substrate-based COB-WLED emitters. Further extensive experimental investigations on different LED packages are needed to estimate interactions which can influence the lumen output by the packaging parameters.

REFERENCES

[1] E. Juntunen, O. Tapaninen, A. Sitomaniemi et al., “Effect of Phosphor Encapsulant on the Thermal Resistance of a High-Power COB LED Module,” Components, Packaging and Manufacturing Technology, IEEE Transactions on, vol. 3, no. 7, pp. 1148-1154, 2013.

[2] J.-K. Sim, K. Ashok, Y.-H. Ra et al., “Characteristic enhancement of white LED lamp using low temperature co-fired ceramic-chip on board package,” Current Applied Physics, vol. 12, no. 2, pp. 494-498, 2012.

[3] J. S. Kim, S. L. Jeon, D. W. Le et al., “Thermal and Optical Properties of COB Type LED Module Based on Al2O3 and AlN Ceramic Submounts,” Journal of Applied Sciences, vol. 10, pp. 3388-3391, 2010.

[4] EdisonOptoCorp., “Filament series datasheet,” vol. Available "http://www.edison-opto.com.tw/files/product/2014102116512456.pdf".

[5] G. R. Brandes, and J. A. Garceran, "LED light bulbs," US 8596821 B2, US Patents, 2013.

[6] A. Verdes, and Y. Chen, "Light emitting diode (LED) light bulbs," US 6948829 B2, US Patents, 2005.

[7] G. Kim, Y.-C. Shih, J.-P. You et al., “Optical role of die attach adhesive for white LED emitters: light output enhancement without chip-level reflectors,” Journal of Solid State Lighting, vol. 2, no. 1, pp. 1-8, 2015.

[8] J. F. Muth, J. H. Lee, I. K. Shmagin et al., “Absorption coefficient, energy gap, exciton binding energy, and recombination lifetime of GaN obtained from transmission measurements,” Applied Physics Letters, vol. 71, no. 18, pp. 2572-2574, 1997.

[9] J. Kvietkova, L. Siozade, P. Disseix et al., “Optical Investigations and Absorption

Coefficient Determination of InGaN/GaN Quantum Wells," physica status solidi (a), vol. 190, no. 1, pp. 135-140, 2002.

[10] Y.-H. Lin, J. P. You, Y.-C. Lin et al., "Development of High-Performance Optical Silicone for the Packaging of High-Power LEDs," Components and Packaging Technologies, IEEE Transactions on, vol. 33, no. 4, pp. 761-766, 2010.

[11] Y. Shao, Y.-C. Shih, G. Kim et al., "Study of optimal filler size for high performance polymer-filler composite optical reflectors," Optical Materials Express, vol. 5, no. 2, pp. 423-429, 2015/02/01, 2015.

[12] Y.-C. Shih, G. Kim, L. Huang et al., "Role of Transparent Die Attach Adhesives for Enhancing Lumen Output of Midpower LED Emitters With Standard MESA Structure," Components, Packaging and Manufacturing Technology, IEEE Transactions on, vol. 5, no. 6, pp. 731-736, 2015.

[13] M.-H. Chang, D. Das, and M. Pecht, "Junction Temperature Characterization of High Power Light Emitting Diodes." pp. 23-24.

[14] E. R. Dobrovinskaya, L. A. Lytvynov, and V. Pishchik, Sapphire: material, manufacturing, applications: Springer Science & Business Media, 2009.

[15] G. Lu, S. Yang, and Y. Huang, "Analysis on failure modes and mechanisms of LED," Reliability, maintainability and safety, pp. 1237-1241, 2009.

CHAPTER 5

OPTIMAL DESIGN OF QUANTUM DOT COLOR CONVERSION FILM IN LCD BACKLIGHTING

5.1. INTRODUCTION

The pursuit of self-emitting displays such as organic light emitting diodes (OLEDs), which is gradually increasing its market share from mobile application products to larger displays, requires higher performance and higher efficiency than the conventional liquid crystal displays (LCDs) [1, 2]. Especially, since the white light emitting diode (LED), which is mainly used as the conventional LCD backlight, does not satisfy the extended color gamut required by the standards of DCI-P3 [3] or Rec. 2020 [4] suggested for ultra-high definition (UHD) displays, hence it is extremely important to secure the light source with a wide color gamut for LCDs to compete with OLEDs in terms of color gamut. White LEDs (WLEDs) using YAG:Ce-based phosphors boast high efficiency and are well suited for use in general lightings, however those are not suitable for use in displays backlighting because the large portion of the spectrum is blocked by color filters on top of the LCD panel [5]. For more efficient backlighting, red, green, and blue peak wavelengths that match with the wavelengths of the color filter are required. In the case of conventional inorganic phosphors, a wide color gamut cannot be obtained due to the wide full width half maximum (FWHM) of the green phosphor [6]. Therefore, more advanced photonic materials for replacing

conventional phosphors have been researched, and quantum dots (QDs) are one of the attracting approaches [7]. The advantages of QDs of adjustable peak wavelengths and narrower FWHM provide the LCD with better performance than WLEDs using conventional phosphors [8]. One of the critical reasons for the QDs not widely used is that QDs are unstable nanoparticles compared to conventional phosphors [9]. The external quantum efficiency (EQE) of the QDs are known to be severely degraded under exposure of heat and humidity, and this results in long-term reliability problems. Therefore, it is regarded that QDs cannot effectively replace existing phosphors. Thus, recent research activities have focused on improving the packaging of QD materials to effectively isolate from heat and moisture sources [10]. In the case of the initial QD-based LED backlight, on-chip QD packaging, which directly replaces the phosphor, has been used. However, it was difficult to avoid the deterioration of the efficiency due to long-term driving because the QD material is in contact with the LED die, which is a heat source. Since then, QD-based LED backlight research has been developed as a remote color conversion layer structure and it can be divided into on-edge type QD tube and on-surface type QD film [11]. In case of larger displays, on-surface type QD film is more advantageous than on-edge type QD tube because there is a problem for QD tube of uniform color distribution toward the large screen display. In addition, the QD film is the most advantageous in terms of long-term reliability because the distance from the LED die is the farthest, which is the heat source. One disadvantage for the QD film is that the amount of QD materials required for the QD film is increasing dramatically compared to the on-chip QD-LED or QD tube as the area of the display increases, which leads to an increase of manufacturing cost. Therefore, the QD film packaging technology that reduces the amount of QD materials used while maintaining the targeted color coordinate is very important in

terms of manufacturing cost reduction and QD material supply and demand [12]. Recycled blue emission by using a dichroic filter is attracting attention as a suitable technique for dilute QD film packaging because it improves the color conversion efficiency by QD materials [13]. However, the study of optimizing the amount of recycled blue emissions for the maximized optical output at the same time as the targeted color coordinate has not been studied in detail yet, and less attention is also paid to how the dichroic filter affects the packaging parameters of the backlight unit such as backlight reflector. In this paper, it is demonstrated for the first time that a dichroic filter on the QD color conversion film can be optimized in terms of its blue emission transmittance, which results in a reduction of over 30% of the amount of QD materials required, while maintaining the targeted color coordinate, color gamut and the optical output of the backlight. In addition, it is found for the first time, that there is a strong impact of the reflectance of the backlight reflector on the optical output when a dichroic filter is employed. The significant implication of the present simulation results to the optimal design of more efficient backlight for LCDs, is outlined.

5.2. APPROACH

Figure 5.1 depicts the schematic cross-sectional view of a 6-inch liquid crystal display with QD color conversion film and dichroic filter which is made of multiple stack of dielectric layers with a combination of high and low refractive indices in order to obtain a selectivity in transmission and reflection spectra. Reflected part of blue emission is recycled within the light guide plate (LGP) and therefore the color conversion efficiency by the QD conversion film is expected to be enhanced. Light intensity is simulated on the

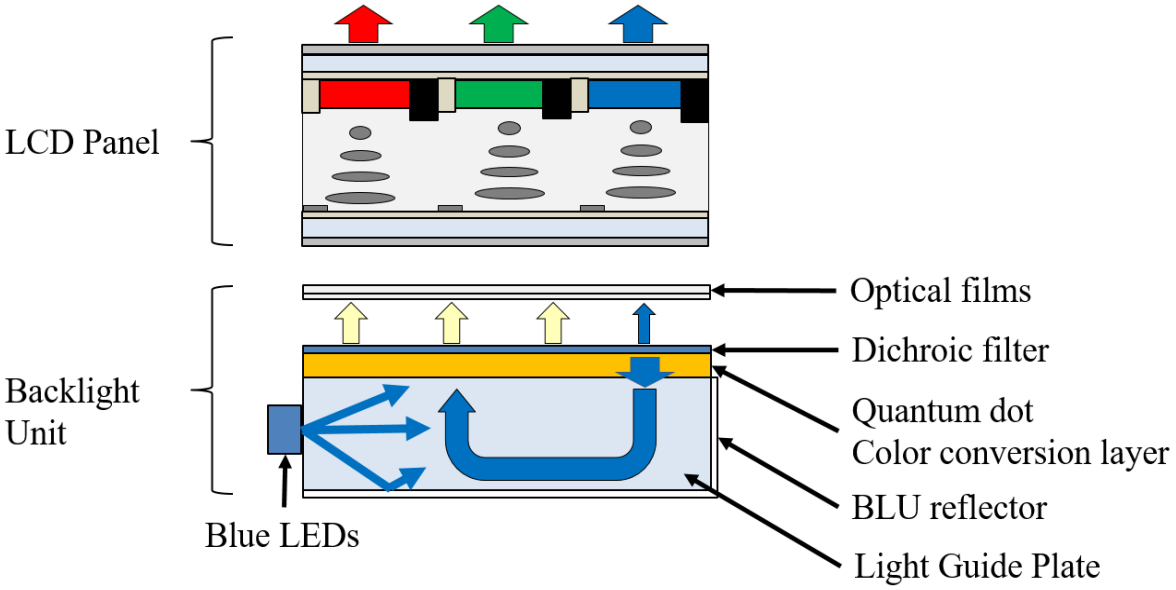

Figure 5.1. Schematic cross-sectional drawing of a liquid crystal display with QD color conversion film and dichroic filter used in simulation. For the backlight unit, an edge-lit blue LED array is located on the side of the light guide plate (LGP). The LGP is surrounded by reflection layers on the side and the bottom, which performs diffusive reflection dominant.

backlight unit (BLU) level, and a whole display including color filters, polarizers and the liquid crystal layer is considered in order to obtain a color gamut [14, 15]. An edge-lit blue LED array is located on the side of the light guide plate. Eight blue LED emitters (0.5 W in output power each) with a peak wavelength of 450 nm were used in the LED array. The LGP is surrounded by a BLU reflector on the side and the bottom, which performs diffusive reflection dominant [16, 17]. The maximum reflectance of the reflective layer is set of 99 % and ranged from 88 % to 99 % to investigate the influence on the optical output of LCD backlight, which is associated with dichroic filter. On-surface type QD color conversion film is placed above the LGP, and the absorption and photoluminescence spectra of green and red QDs are carefully modeled based on the measured data [7]. The thickness of the QD film is set of 100 microns. Peak wavelengths of green and red emission after color conversion were targeted at 535 nm and 625 nm, respectively. The color coordinate of the targeted white emission after color conversion was optimized at (0.231, 0.244) in CIE 1931 for LCD backlight. Figure 5.2a presents the angular dependence of the transmittance spectra for a low-band reflecting dichroic filter which is commercially available, at the incident angle ranging from 0 degree to 45 degrees [18]. Fig 2b presents the transmission spectra of the dichroic filters at normal incident angle used in this study. The reflection spectra are automatically calculated by using $R + T = 1$. The angular dependence of the transmission and reflection spectra for each dichroic filter is also applied on each model. The thickness of the dichroic filter is set of 50 microns. For the optimization of the recycled blue emission, the transmittance spectra for the blue region of each dichroic filter modeled was adjusted from 50% to 80% for a peak wavelength of 450 nm in terms of the normal incident angle. To elucidate the detailed impact of packaging processes and materials, Monte-Carlo

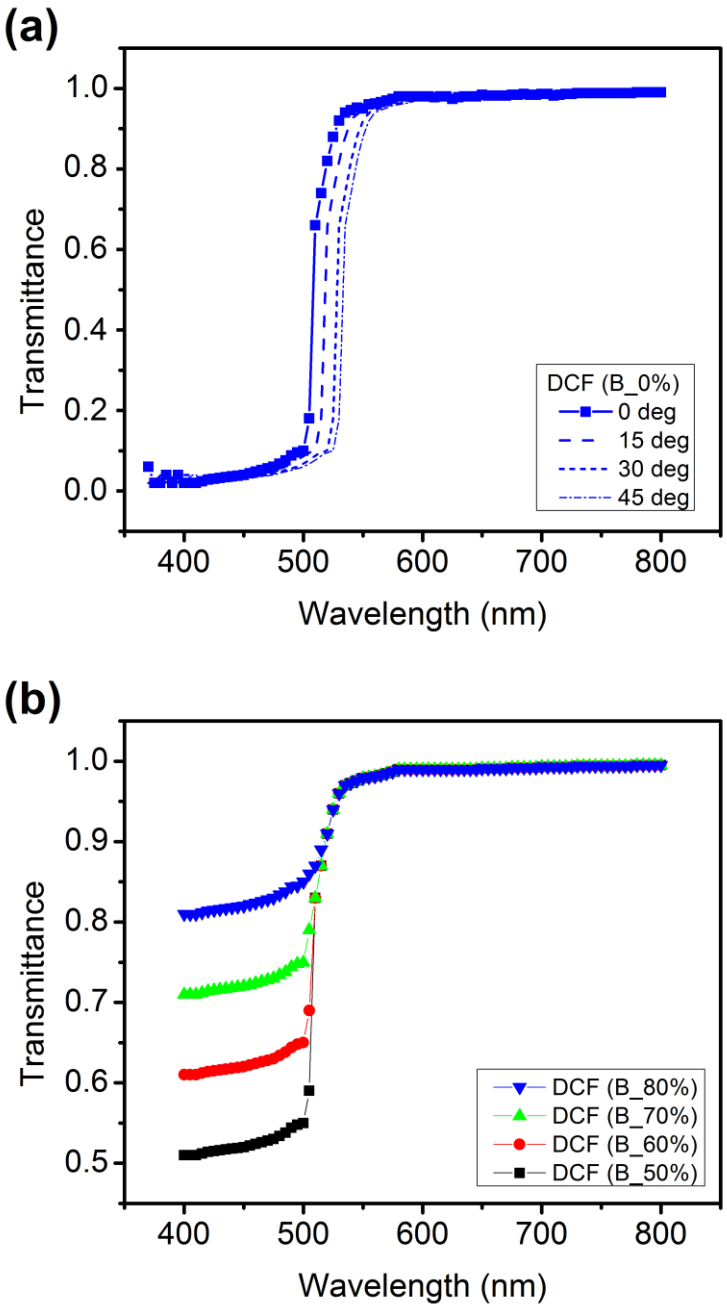

Figure 5.2. Transmission spectra of dichroic filters. (a) Transmittance of the dichroic filter with 0 % of blue transmission, at the incident angle ranging from 0 degree to 45 degrees and (b) Transmittance of the blue emission region is set of 50 % (black), 60 % (red), 70 % (green), and 80 % (blue) at normal incident angle

simulations using *LightTools 8.0.3* are employed, and 2,000,000 rays are traced to control simulation error to be less than 1 % for each simulation run.

5.3. RESULT AND DISCUSSION

Figure 5.3a presents the light intensity spectra of the backlight using on-surface type QD color conversion film. For the QD film without dichroic filter, and the concentrations of green and red QDs are 12.0 wt% and 5.7 wt%, respectively. The power conversion efficiency (PCE) is 52.2 $lm \cdot W^{-1}$. Optimization of the parameters were carried out to obtain the matched color coordinate and luminous output with QD film using a dichroic filter. By ranging the transmittance of blue emission from 50 % to 80 % to find an optimal transmittance of blue emission for the dichroic filter, the amount of green and red QDs are also carefully controlled to maintain green and red peaks. It was initially expected that the more of blue emission is recycled by using a dichroic filter, the more of green and red emissions to be converted. However, the results show that the amount of green and red QDs are not effectively reduced with the dichroic filter of 50 % transmission for the blue emission to match the targeted white point and to maintain luminous output at the same time, even though that case reduces the amount of green and red QDs by almost 40 % to match the green and red emissions. Blue peak remained lower than the targeted peal level, a substantial part of the recycled blue emission could be lost while the recycling process in the BLU. The same level of blue emission is observed when the dichroic filter of which the transmittance for the blue emission is 80 % is used, and reduced amount of green and red QDs under that condition which is to match with one without dichroic filter were 25 % and 33 %, respectively. Resulted color coordinates for blue, green, and red peaks from simulations are (0.143, 0.035),

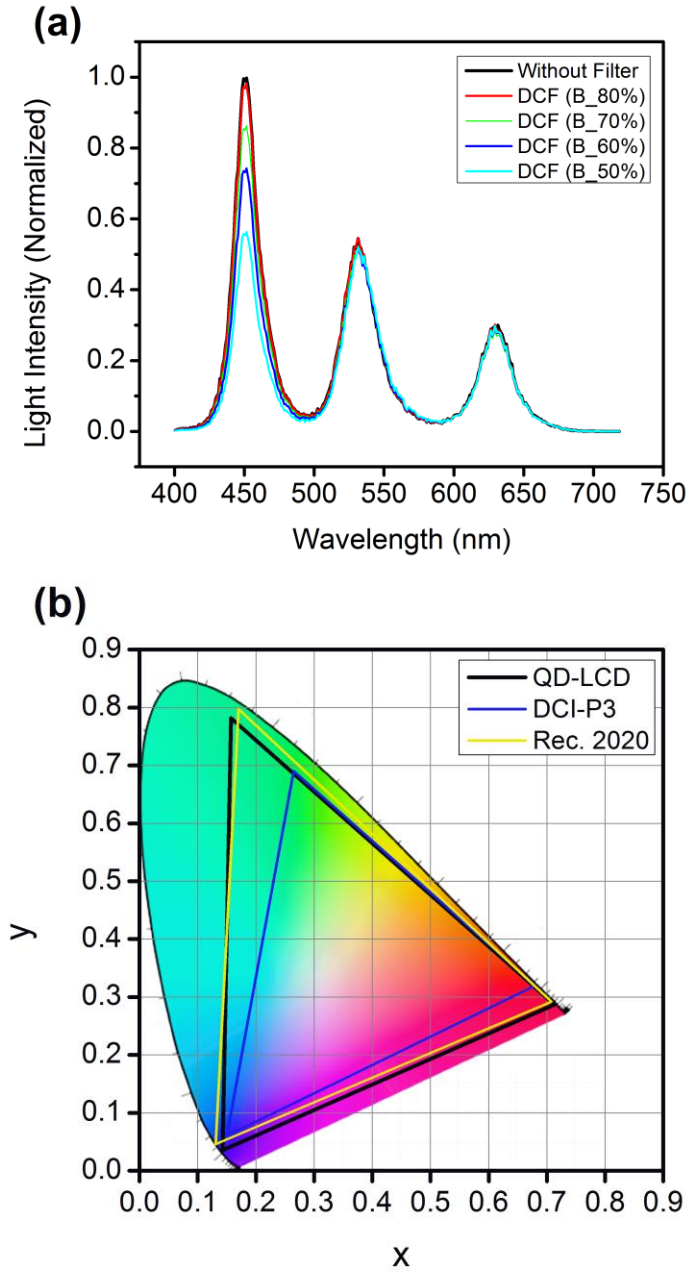

Figure 5.3. (a) Light intensity spectra of LCD backlight using QD color conversion film without dichroic filter (black), and with dichroic filter of which the transmittance of blue emission is 80 % (red), 70 % (green), 60 % (blue), and 50 % (cyan). The concentration of green and red QDs are 12.0 wt% and 5.7 wt% (without filter), respectively, and 9.0 wt % and 3.8 wt% (with dichroic filter), respectively. (b) CIE 1931 color gamut of optimized LCD using the BLU with the QD film and the dichroic filter (black) compared to DCI-P3 (blue) and Rec. 2020 (yellow).

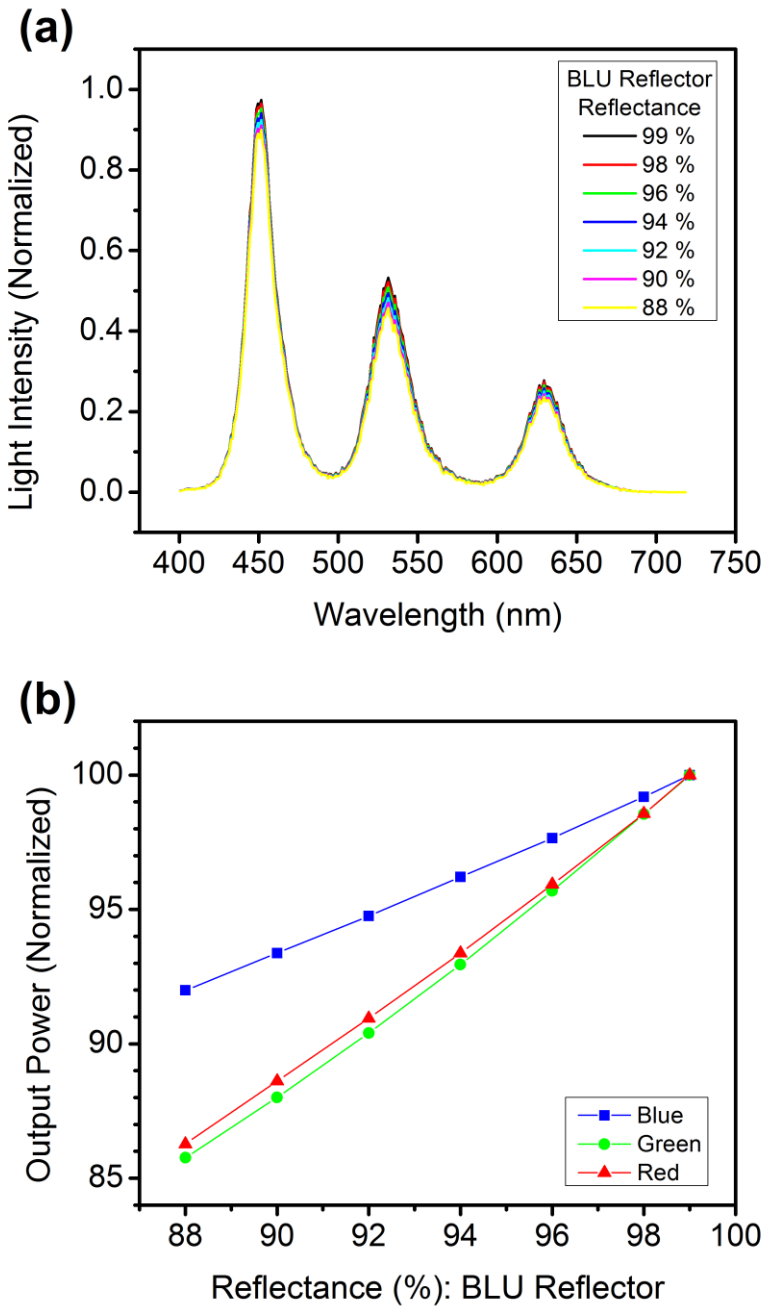

Figure 5.4. (a) light intensity spectra of the LCD backlight using QD film and dichroic filter by the reflectance of the backlight reflector. The blue emission transmittance for the dichroic filter is fixed at 80%. The range of the reflectance of the backlight reflector is from 88 % to 99 %. (b) Optical power separated as blue, green, and red emissions dependent on the reflectance of the backlight reflector.

(0.157, 0.782), and (0.713, 0.287), respectively. Figure 5.3b presents the color gamut of the finally optimized LCD using the BLU with the QD film and the dichroic filter (denoted as QD-LCD) compared to other standards of DCI-P3 and Rec. 2020. The color gamut in terms of the area ratio obtained is 138.8 % of the DCI-P3 and 99.6 % of the Rec. 2020. There is an offset is observed between the QD-LCD and the Rec. 2020, the color gamut in terms of the coverage ratio of the QD-LCD is 94.2 % of the Rec. 2020. This reduced amount of QD material, while maintaining its color gamut and optical output would lead to a significant reduction in manufacturing costs, especially for larger area displays backlight [12].

Since a portion of the blue emission is recycled when the dichroic filter is used, it can be expected that the reflection and absorption inside the backlight unit will have a significant impact on the optical output when compared to the QD film without a filter. Figure 5.4a presents the difference in light intensity by the reflectance of the backlight reflector. The blue emission transmittance of the dichroic filter was fixed at 80 % for all plots. It is observed that all blue, green, and red emissions are reduced as the reflectance of the BLU reflector decreased from 99 % to 88 %. The effect of reduced reflectance of the BLU reflector on each blue, green, and red emissions are presented in Figure 5.4b. The optical output for each band is separated and integrated from 400 nm to 491 nm (blue), from 491 nm to 591 nm (green), and from 591 nm to 730 nm (red). The plots show that the blue emission is reduced by 8 % while the green and red emissions reduced by 14.2 % and 13.7 %, respectively. This means that the more of blue emission is recycled with a dichroic filter, the converted green and red emissions are influenced further by the parameters inside the backlight, especially for the reflectance of the BLU reflector. In terms of the luminous output for the white emission, it is reduced by 13.9 % as the reflectance of BLU reflector is decreased from 99 % to 88%.

However, the white point chromaticity is only shifted from (0.231, 0.244) to (0.228, 0.234). This could be regarded as a minor shift, but it could imply that the concentration of the green and red QDs should be controlled carefully to target a white balance due to the discrepancy of the effect for each band by the reflectance of the BLU reflector. Therefore, it is indispensable to maximize the light utilization efficiency by designing a more efficient backlight unit and accomplish the reduction in the concentration of QD materials by using a dichroic filter.

5.4. CONCLUSION

In this work, a design optimization to reduce usage of QD materials for the LCDs backlight has been suggested. By using a dichroic filter with the optimized blue emission transmittance, a substantial amount of green and red QDs can be reduced, while maintaining the targeted color coordinate, color gamut and the optical output of the backlight. A strong effect of the reflectance of the backlight reflector on the optical output when using a dichroic filter is also investigated. Although this study focuses on simulations to systemize the parameters, the findings may well have a bearing on influences in design of more efficient backlight for LCDs. Further extensive experimental investigations on different LED arrays and configurations for the backlight are needed to estimate interactions which can influence the optical performances by the packaging parameters.

REFERENCES

[1] C.-H. Chang, H.-C. Cheng, Y.-J. Lu et al., “Enhancing color gamut of white OLED displays by using microcavity green pixels,” Organic Electronics, vol. 11, no. 2, pp. 247-254,

2010.

[2] X. Chen, Y. Chen, Z. Ma et al., "How is energy consumed in smartphone display applications?." p. 3.

[3] C. Poynton, “Wide-gamut displays,” Information Display, vol. 23, no. 7, pp. 10, 2007.

[4] J. M. Hillis, J. Thielen, J. Tibbits et al., "17.1: Invited Paper: Closing in on Rec. 2020: How Close Is Close Enough?." pp. 223-226.

[5] P. Pust, P. J. Schmidt, and W. Schnick, “A revolution in lighting,” Nat Mater, vol. 14, no. 5, pp. 454-458, 2015.

[6] T. Takeda, N. Hirosaki, S. Funahshi et al., “Narrow-Band Green-Emitting Phosphor Ba2LiSi7AlN12:Eu2+ with High Thermal Stability Discovered by a Single Particle Diagnosis Approach,” Chemistry of Materials, vol. 27, no. 17, pp. 5892-5898, 2015/09/08, 2015.

[7] E. Jang, S. Jun, H. Jang et al., “White-Light-Emitting Diodes with Quantum Dot Color Converters for Display Backlights,” Advanced Materials, vol. 22, no. 28, pp. 3076-3080, 2010.

[8] J. Chen, J. Hartlove, V. Hardev et al., "P-119: High Efficiency LCDs using Quantum Dot Enhancement Films." pp. 1428-1430.

[9] P. Bhattacharya, S. Ghosh, and A. Stiff-Roberts, “Quantum dot opto-electronic devices,” Annu. Rev. Mater. Res., vol. 34, pp. 1-40, 2004.

[10] M. Molaei, M. Marandi, E. Saievar-Iranizad et al., “Near-white emitting QD-LED based on hydrophilic CdS nanocrystals,” Journal of Luminescence, vol. 132, no. 2, pp. 467-473, 2012.

[11] S. Coe-Sullivan, W. Liu, P. Allen et al., “Quantum dots for LED downconversion in

display applications," ECS Journal of Solid State Science and Technology, vol. 2, no. 2, pp. R3026-R3030, 2013.

[12] J. S. Steckel, R. Colby, W. Liu et al., "68.1: Invited Paper: Quantum Dot Manufacturing Requirements for the High Volume LCD Market," SID Symposium Digest of Technical Papers, vol. 44, no. 1, pp. 943-945, 2013.

[13] C. You, J. Qi, F. C. Hsu et al., "Quantum Dot-Enhanced Display Having Dichroic Filter," US20160070137 A1, US Patent, 2016.

[14] Z. Luo, Y. Chen, and S.-T. Wu, "Wide color gamut LCD with a quantum dot backlight," Optics Express, vol. 21, no. 22, pp. 26269-26284, 2013.

[15] R. Zhu, Z. Luo, H. Chen et al., "Realizing Rec. 2020 color gamut with quantum dot displays," Optics Express, vol. 23, no. 18, pp. 23680-23693, 2015/09/07, 2015.

[16] Y. Shao, and F. G. Shi, "Exploring the critical thickness for maximum reflectance of optical reflectors based on polymer-filler composites," Optical Materials Express, vol. 6, no. 4, pp. 1106-1113, 2016/04/01, 2016.

[17] Y. Shao, Y.-C. Shih, G. Kim et al., "Study of optimal filler size for high performance polymer-filler composite optical reflectors," Optical Materials Express, vol. 5, no. 2, pp. 423-429, 2015/02/01, 2015.

[18] Y. Wu, D. Zhang, J. M. Russo et al., "Optical Performance of Dichroic Filters in Solar Spectrum-Splitting application," OSA Technical Digest (online). p. JM3A.17.

CHAPTER 6

COST-EFFECTIVE NOVEL DESIGN OF QUANTUM DOT COLOR CONVERSION FILMS FOR COLOR FILTER REPLACEMENT IN WIDE COLOR GAMUT LCD AND OLED DISPLAYS

6.1. INTRODUCTION

The quantum dot (QD) based color conversion is actively investigated not only for liquid crystal displays (LCDs) but also for organic light emitting displays (OLEDs) with a wide color gamut (WCG) [1-4], due to its tunable wavelengths and narrow full width half maximum (FWHM) [5-8]. However, a reduction in the amount of QD content in the QD-embedded color conversion film is required for cost reduction [9, 10]. One method investigated so far is to replace color filters by patterned QD films, but this approach still faces some structural and optical issues [11-13].

Research activities have reported recently not only the use of QD-based color conversion films with higher conversion efficiency [14], but also designing patterned QD films at the top of the LCDs or OLEDs by replacing color filters to reduce the amount of QD materials used [15]. Among them, the backlight using the remote QD film has already been commercialized, but the approach using the pattern printed QD film has not been sufficiently studied due to some problems. First, there is a difficulty in developing unit processes due to the placement polarizing film. Second, unwanted blue emission leaks from the red and green

QD sub-pixels because the red and green sub-pixels do not completely absorb the blue light. Hence, it is rather required to increase the concentration of the QD materials in each sub-pixel even further to implement WCG, otherwise, color filters or a short-band reflector is still required [11-13], which is not desired.

The objective of the present work is to develop a novel cost-effective design of quantum dot color conversion patterned films for color filter replacement for wide color gamut displays. It is demonstrated a novel cost-effective design of the QD conversion film that can dramatically reduce the amount of QD amount required while maintaining the same conversion efficiency. It is experimentally confirmed that the dispersion of diffusing particles can exhibit the same level of luminous output even when the amount of green and red QD materials used are reduced by 41.7 % and 58.3 %, respectively. By using this novel method, a monochromatic color conversion film of green or red can be implemented. It is also demonstrated for the first time, the color converting sub-pixels can replace conventional color filters for the LCDs. By using Monte-Carlo optical simulations, a uniform color distribution without color distortion with respect to the viewing angle for the improved optical structure can be obtained by using our designed monochromatic color converting sub-pixels.

6.2. APPROACH

Figure 6.1 illustrates the comparison of schematic cross-sectional views of the conventional LCD and the WCG-LCD with patterned QD film with embedded diffusers. An edge-lit white (1a) or blue (1b) LED arrays are located on the side of the light guide plate. Eight blue LED emitters (0.5 W in output power each) with a peak wavelength of 450 nm

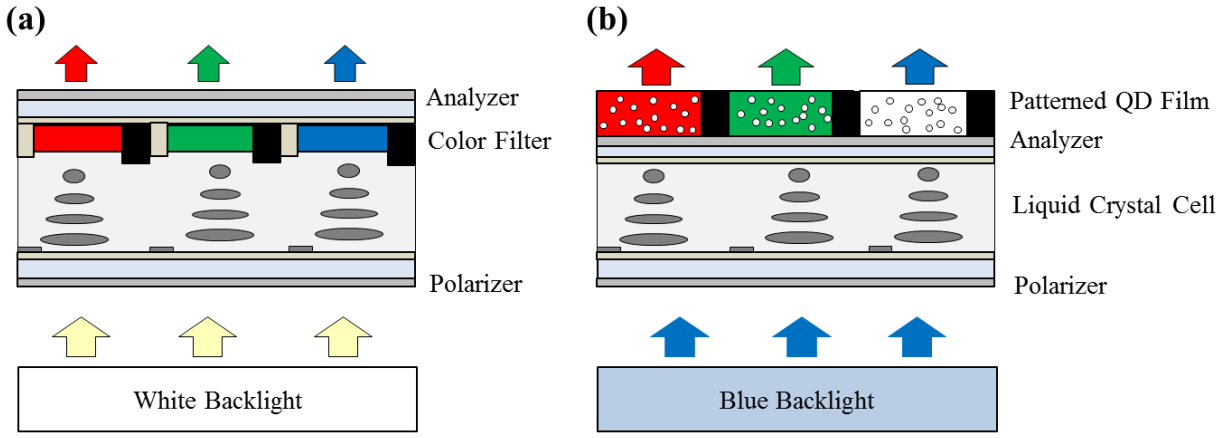

Figure 6.1. Schematic cross-sectional views of (a) conventional LCD and (b) the WCG-LCD using quantum dot-based patterned color conversion film with embedded diffusers. For the blue pixel, only diffusers are dispersed in the transparent matrix since the backlight is blue.

were used in the LED array. The LGP is surrounded by a backlight unit (BLU) reflector on the side and the bottom, which performs diffusive reflection dominant [14]. Unlike the conventional LCD, the analyzer is below the patterned QD film for the WCG-LCD, therefore the polarized blue emission enters the patterned QD film to convert light into red and green. Optically optimized diffusers are dispersed in the QD film to extend light path for the blue emission to be sufficiently absorbed by the QD materials. For the blue sub-pixels, only diffusers are dispersed in the transparent matrix for a wide viewing angle.

To obtain the measurement data, QD-based monochromatic color conversion layers

packaged onto a blue LED emitter (20 mA in input current) with a peak wavelength of 450 nm. Each LED emitter is packaged with silicone resin of which the refractive index is 1.53 at 450 nm for flatted top surface. The green and red QD materials are mixed with a silicone resin matrix and evenly coated onto the LED emitter as a monochromatic color conversion layer. Peak wavelengths of green and red emission after color conversion were targeted at 535 nm and 625 nm, respectively. The concentration of green and red QD material mixed is ranged from 1 wt.% to 18 wt.%, and from 1 wt.% to 24 wt.%, respectively. The thickness of each color conversion layer is 100 microns. For the diffusers dispersed in the QD color conversion film, the TiO2 powder is used for experimental measurement. To optimize the optical parameters for the diffusing particles, Monte-Carlo optical simulations using *LightTools 8.0.3* are employed. Traced rays of 2,000,000 are assigned to control simulation error to be less than 1 % for each simulation run. Rrefractive index of the diffusers is ranged from 1.7 to 2.6 at 450 nm of the wavelength, and the diameter is ranged from 25 nm to 500 nm. The light intensity is simulated on the BLU level, and a whole display including patterned QD film, polarizers and the liquid crystal layer is considered to obtain a color gamut for comparison.

6.3. RESULT AND DISCUSSION

Figure 6.2a presents the emission spectra of green monochromatic QD color conversion film as a function of the concentration of QD materials. The result shows that 18 wt.% of green QD is required to obtain a monochromatic green color conversion film using blue light source. The range of double the FWHM for each peak wavelength of blue and green emission are taken and integrated to plot a normalized color conversion as shown in Figure

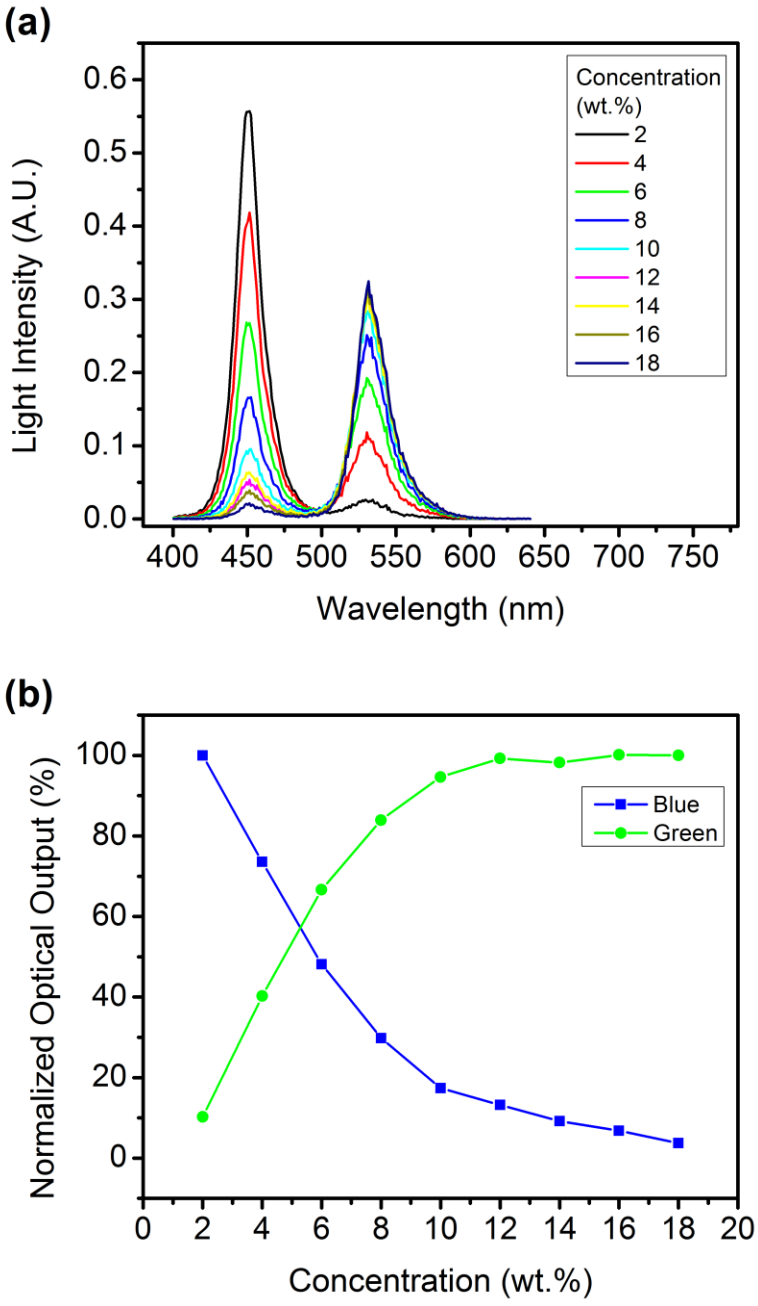

Figure 6.2. (a) Emission spectra of green monochromatic QD color conversion film, (b) normalized optical output by color conversion of green QD

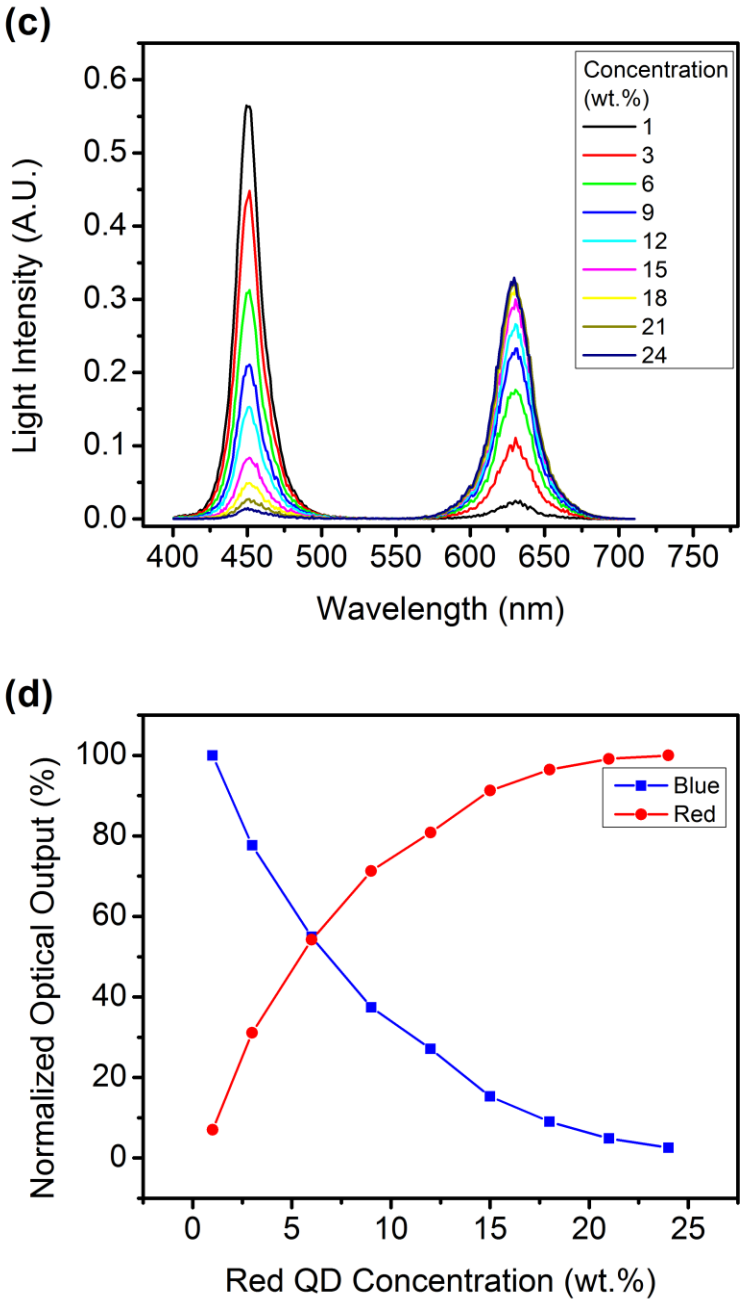

(c) Emission spectra of red monochromatic QD color conversion film, (d) normalized optical output by color conversion of red QD as a function of weight concentration of QD materials.

6.2b. It shows that the green emission reaches its maximum at the concentration of 12 wt.% and saturated. However, the more green-QD material is required to eliminate blue emission to achieve a monochromatic green emission. The emission spectra of red monochromatic QD color conversion film with the same settings is presented in Figure 6.2c and Figure 6.2d. Likewise, the red emission is saturated at which the blue emission leaks, and therefore additional red QD material is required to suppress unwanted blue emission. The role of additional QD materials for each color conversion film is increasing chances for blue emission to be absorbed by green or red QD materials, but this additional amount of QD materials don't contribute the color conversion efficiency. Instead of adding more QDs, the inert diffusers can also extend the light path of blue emission so that the enhanced color conversion efficiency for the QD material is expected even with a reduced concentration.

The optical parameters for the diffusers are optimized by using optical simulations. The absorption and emission spectra of green and red QD materials are plugged in the simulation model to proceed optimization process. Fig 6.3 presents the optimized refractive index and diameter for diffusers. It is evident that the contrast of refractive indices between the matrix and the diffuser material is the key for green QD based color conversion films as shown in Figure 6.3a. By taking the refractive index of 2.6, the diffusers of which the concentration of 5 wt.% effectively extend light path of blue emission and eliminate it while the green emission to maintain with the concentration of green and red QDs are dramatically reduced by 41.7 % and 58.3 %, respectively, compared to ones without diffusers. The effect of the diameter of the diffusing particle on the color conversion efficiency for the green QD is presented in Figure 6.3b. By ranging its diameter from 25 nm to 500 nm, the minimum of blue emission is found at 100 nm. However, the optimized diameter is 50 nm because the

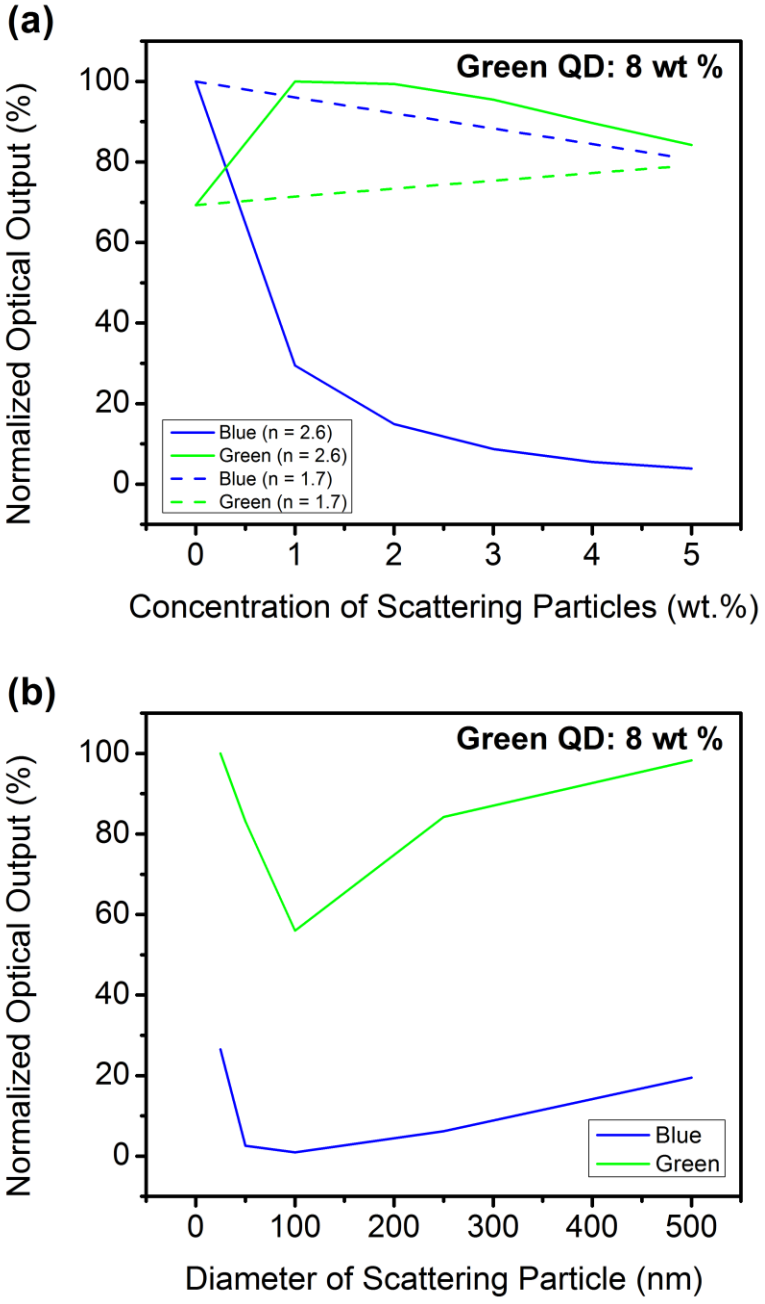

Figure 6.3. Optimization process of green and red QD-based monochromatic color conversion films using diffusers. Normalized optical output of blue and (a) green emission as a function of weight concentration of diffusers with different refractive indices, (b) green emission as a function of diameter of diffusers

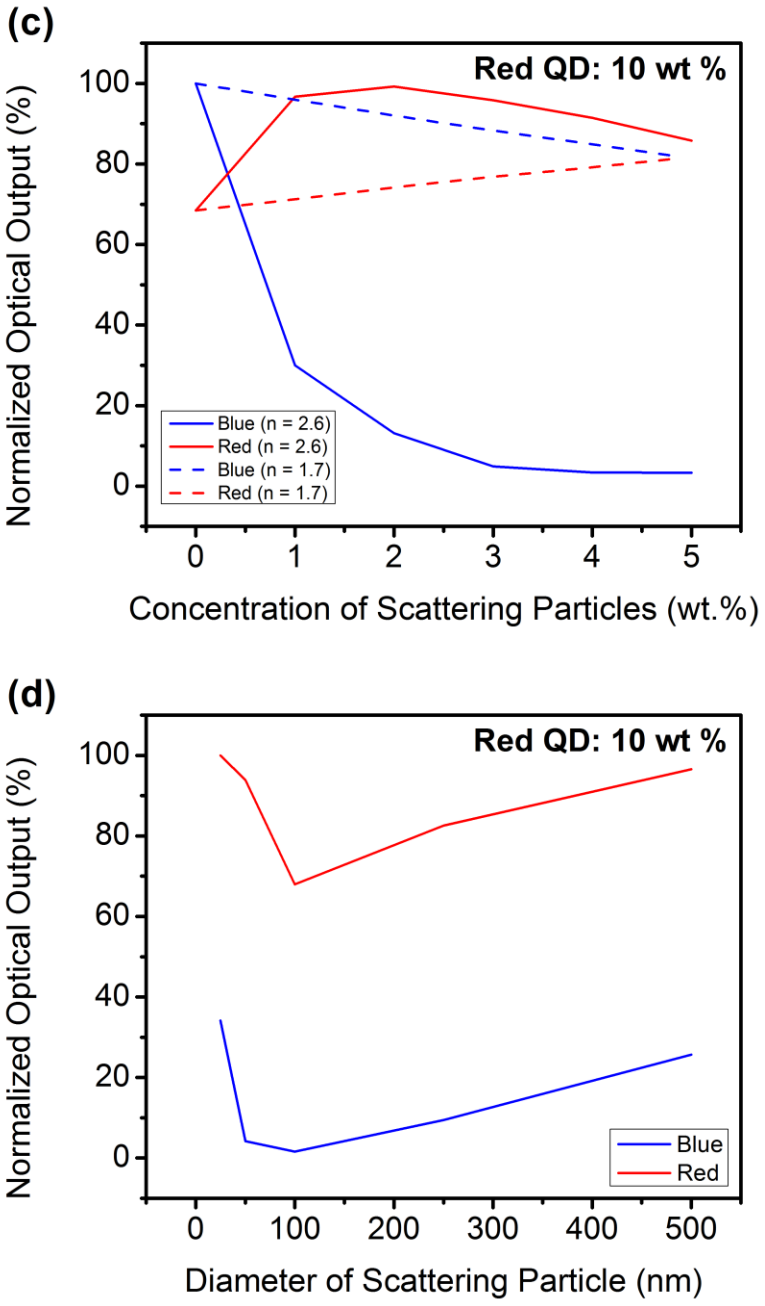

(c) red emission as a function of weight concentration diffusers with different refractive indices, (d) red emission as a function of diameter of diffusers.

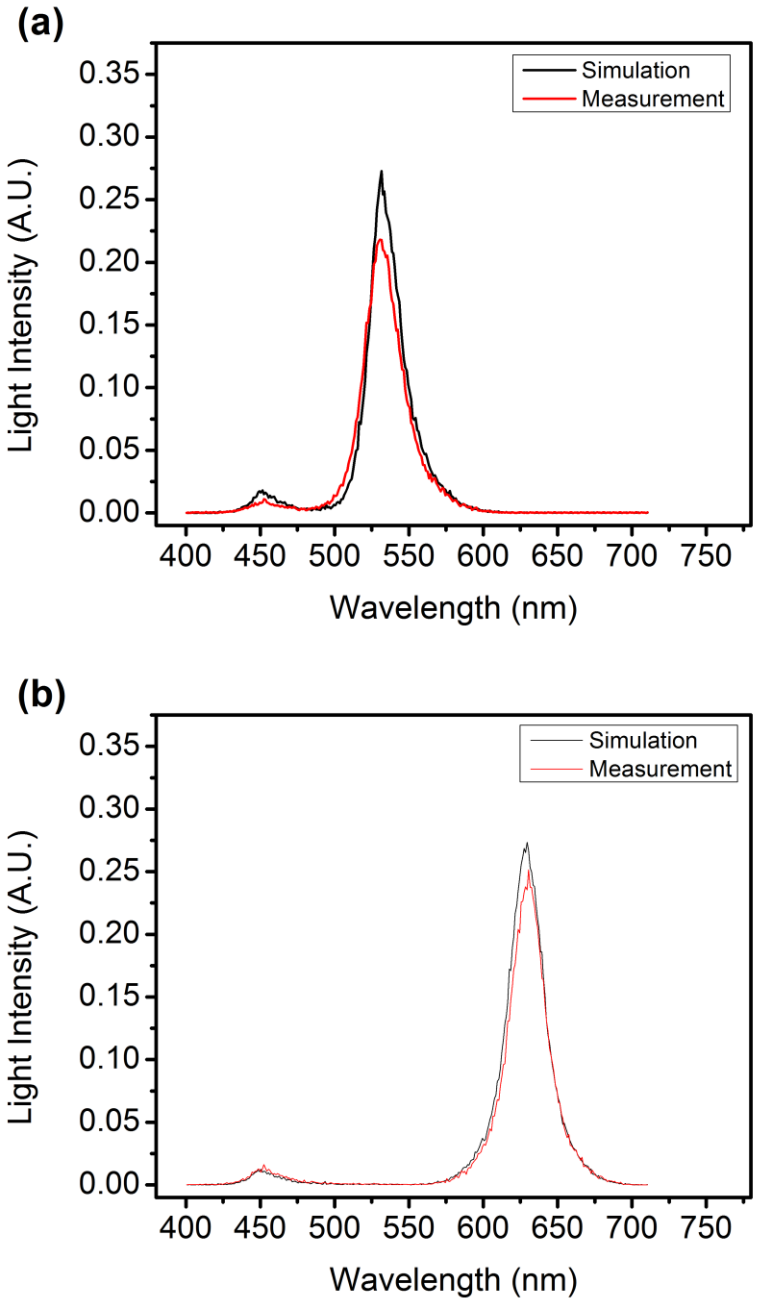

Figure 6.4. Comparison of emission spectra of monochromatic color conversion film with embedded diffusers using (a) green QD and (b) red QD

level of green emission is higher than 100 nm. We carried out the same optimization process with the red QD, and the concentration of red QD is reduced by 58 % at the same refractive index and size of the diffusers. Figure 6.4 presents the emission spectra of green and red monochromatic color conversion film using TiO2 diffusers with the diameter of 50 nm up to 5 wt.%. The measurement shows a good agreement with the simulation results.

We confirmed that the monochromatic color conversion can be achieved with a dramatically reduced amount of QD. This structure can be applied to the development of LCDs and OLEDs having improved optical characteristics. Conventional LCDs have a structure in which a white light source as a backlight and the white light passing through a liquid crystal panel, and some OLED applications also form color displays using color filters on white OLEDs. White backlight passes through color filters to produce red, green, and blue emission. The limitations of these structures are (1) one thirds of incident light is blocked by color filters, (2) a decrease in the light utilization efficiency due to the polarizer located at both ends of the liquid crystal panel, in case of the LCDs. The light passing through the color filter passes through the polarizer and the luminance is lowered, causing a difference in color and luminosity depending on the viewing angle. Replacing a color filter by RGB patterned monochromatic color conversion films could be free of these problems. A comparison of the two types of LCD structures is shown in Figure 6.1.

The advantage of the improved structure is that it can achieve even better optical properties in less than a half of the amount of QD materials rather than conventional QD-based color conversion films. In addition, uniform angular distribution of light becomes possible by patterned color converting subpixels due to the scattering. The optical simulation results using the improved structure are shown in Figure 6.5. The result shows

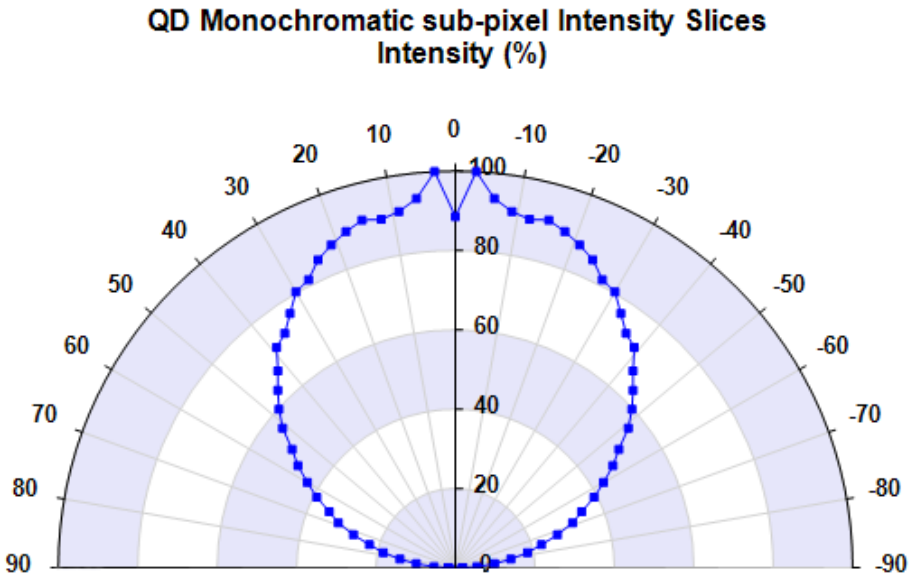

Figure 6.5. Angular intensity distribution for the LCD using QD-based monochromatic color converting sub-pixels with embedded diffusers.

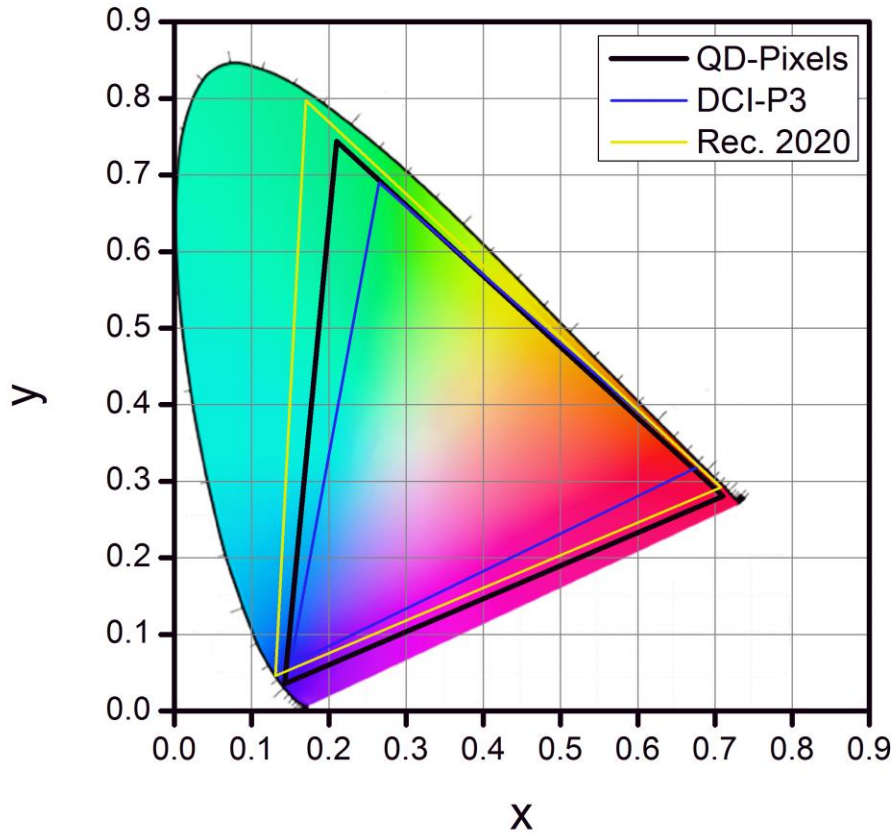

Figure 6.6. Color gamut of the LCD using QD-based monochromatic color converting sub-pixels with embedded diffusers compared to DCI-P3 and Rec.2020

that the light passing through the monochromatic color converting subpixel structure exhibits a Lambertian light distribution. Due to the narrow FWHM of QD materials, WCG can be obtained even in an LCD structure without color filters, and as shown in Figure 6.5b, the color gamut of the LCD with monochromatic color converting sub-pixels obtained is 126.8 % of the DCI-P3 and 91 % of the Rec. 2020.

6.4. CONCLUSION

In this study, a cost-effective method for monochromatic color conversion film using QD materials was obtained. It was confirmed by light simulation and experimental measurement that a small number of diffusers can save a significant amount of QD materials used while maintaining the same color conversion efficiency. In addition, we have confirmed that color converting sub-pixels that can be applied to advanced not only LCDs but also OLEDs can show better optical characteristics than conventional displays. Further continuous and extensive experimental investigations on the advanced LCDs and OLEDs structure using QD-based monochromatic color converting sub-pixels are required to figure out its feasibility and reliability.

REFERENCES

[1] Z. Luo, Y. Chen, and S.-T. Wu, “Wide color gamut LCD with a quantum dot backlight,” Optics Express, vol. 21, no. 22, pp. 26269-26284, 2013/11/04, 2013.

[2] J. M. Hillis, J. Thielen, J. Tibbits et al., "17.1: Invited Paper: Closing in on Rec. 2020: How Close Is Close Enough?." pp. 223-226.

[3] R. Zhu, Z. Luo, H. Chen et al., “Realizing Rec. 2020 color gamut with quantum dot

displays," Optics Express, vol. 23, no. 18, pp. 23680-23693, 2015/09/07, 2015.

[4] C. Poynton, "Wide-gamut displays," Information Display, vol. 23, no. 7, pp. 10, 2007.

[5] R. J. Johnson, "Led-based LCD backlight with extended color space," Google Patents, 2003.

[6] M. Anandan, "Progress of LED backlights for LCDs," Journal of the Society for Information Display, vol. 16, no. 2, pp. 287-310, 2008.

[7] E. Jang, S. Jun, H. Jang et al., "White-Light-Emitting Diodes with Quantum Dot Color Converters for Display Backlights," Advanced Materials, vol. 22, no. 28, pp. 3076-3080, 2010.

[8] X. Yuan, J. Hua, R. Zeng et al., "Efficient white light emitting diodes based on Cu-doped ZnInS/ZnS core/shell quantum dots," Nanotechnology, vol. 25, no. 43, pp. 435202, 2014.

[9] S. Coe-Sullivan, W. Liu, P. Allen et al., "Quantum dots for LED downconversion in display applications," ECS Journal of Solid State Science and Technology, vol. 2, no. 2, pp. R3026-R3030, 2013.

[10] J. S. Steckel, R. Colby, W. Liu et al., "68.1: Invited Paper: Quantum Dot Manufacturing Requirements for the High Volume LCD Market," SID Symposium Digest of Technical Papers, vol. 44, no. 1, pp. 943-945, 2013.

[11] J.-P. Yang, E.-L. Hsiang, and H.-M. Philip Chen, "4-3: Wide Viewing Angle TN LCD Enhanced by Printed Quantum-Dots Film," SID Symposium Digest of Technical Papers, vol. 47, no. 1, pp. 21-24, 2016.

[12] H.-J. Kim, M.-H. Shin, J.-S. Kim et al., "61-2: Optical Efficiency Enhancement in Wide Color Gamut LCD by a Patterned Quantum Dot Film and Short Pass Reflector," SID

Symposium Digest of Technical Papers, vol. 47, no. 1, pp. 827-829, 2016.

[13] Y. Liu, J. Lai, X. Li et al., “A Quantum Dot Array for Enhanced Tricolor Liquid-Crystal Display,” IEEE Photonics Journal, vol. 9, no. 1, pp. 1-7, 2017.

[14] G. Kim, Y. C. Shih, and F. G. Shi, “Optimal Design of a Quantum Dot Color Conversion Film in LCD Backlighting,” IEEE Journal of Selected Topics in Quantum Electronics, vol. 23, no. 5, pp. 1-4, 2017.

[15] H. J. Kim, M. H. Shin, H. G. Hong et al., “Enhancement of Optical Efficiency in White OLED Display Using the Patterned Photoresist Film Dispersed With Quantum Dot Nanocrystals,” Journal of Display Technology, vol. 12, no. 6, pp. 526-531, 2016.

CHAPTER 7

SUMMARY AND CONCLUSIONS

The demand of solid state lightings applications such as LEDs is rapidly increasing, and cost-effective manufacturing technology with higher optical performance and reduced power consumption is crucial for the LEDs to replace conventional light sources in the lightings market. The first chapter briefly introduces the basic outline of LED manufacturing technology. The cost reduction is required for the LEDs continuously and this challenges the novel technologies to be adopted on. Optical performance management has not been considered enough whereas the thermal management has been extensively studied so far. Luminous output for the LED is one of the most important features, however no less important, wide color gamut especially for the displays applications is crucial to comply future standards.

In chapter 2, it is demonstrated that the role of the backside reflector (BR) for the LED chip can be diminished when the optically transparent die attach adhesive (DAA) is used and other key packaging materials and processes are optimized for the leadframe based LED emitters. The light output for a packaged LED emitter with a BR-free chip can be as high as that of the packaged emitter using the same chip but with an added BR.

In chapter 3, the role of the DAAs in influencing light output of the white chip-on-board (COB) LED emitters is investigated. It is demonstrated for the first time that the use of an optically transparent DAA for replacing conventional adhesive for multiple COB white LED emitters leads

to a significant enhancement in light output of up to 22 %. An optimization of packaging materials and process for multiple COB LED emitter to enhance optical efficiency is also studied.

In chapter 4, an investigation of possible packaging and materials optimization of this new type WLED linear array with on objective of maximizing its lumen output. It is found that the lumen output is greatly enhanced up to 26 %. if the transparent substrate is optimized with respect to its dimensions. It is also found that the optically transparent die attach adhesive is preferred over optically reflective one. In addition, an optimization of the refractive index of the DAA, as well as optimization of die spacing and phosphor layer structure contribute significantly in enhancing the lumen output.

In chapter 5, the design of the quantum dot-based color conversion film in the LCD backlighting is optimized in terms of reducing the required amount of relatively expensive QD materials. It is demonstrated for the first time that a dichroic filter on the QD color conversion film can be optimized in terms of its blue emission transmittance, which results in a reduction of over 30% of the amount of QD materials required, while maintaining the targeted color coordinate, color gamut and the optical output of the backlight. In addition, it is studied that there is a strong impact of the reflectance of the backlight reflector on the optical output when a dichroic filter is employed. The significant implication of the present simulation results to the optimal design of more efficient backlight for LCDs is outlined.

In chapter 6, it is demonstrated that the QD-based monochromatic color converting sub-pixels can replace conventional color filters for the displays without optical filters, and a wide color distribution without color distortion with respect to the viewing angle can be obtained as well. Furthermore, the amount of QDs used in the color conversion film for replacing conventional

color filters can be reduced up to 58.3 % by employing optimized diffusers in the film while maintaining its color conversion efficiency.